

Seamless and Energy Efficient Maritime Coverage in Coordinated 6G Space-Air-Sea Non-Terrestrial Networks

Sheikh Salman Hassan, *Student Member, IEEE*, Do Hyeon Kim, Yan Kyaw Tun, *Member, IEEE*, Nguyen H. Tran, *Senior Member, IEEE*, Walid Saad, *Fellow, IEEE*, and Choong Seon Hong, *Senior Member, IEEE*

Abstract—Non-terrestrial networks (NTNs), which integrate space and aerial networks with terrestrial systems, are a key area in the emerging sixth-generation (6G) wireless networks. As part of 6G, NTNs must provide pervasive connectivity to a wide range of devices, including smartphones, vehicles, sensors, robots, and maritime users. However, due to the high mobility and deployment of NTNs, managing the space-air-sea (SAS) NTN resources, i.e., energy, power, and channel allocation, is a major challenge. The design of a SAS-NTN for energy-efficient resource allocation is investigated in this study. The goal is to maximize system energy efficiency (EE) by collaboratively optimizing user equipment (UE) association, power control, and unmanned aerial vehicle (UAV) deployment. Given the limited payloads of UAVs, this work focuses on minimizing the total energy cost of UAVs (trajectory and transmission) while meeting EE requirements. A mixed-integer nonlinear programming problem is proposed, followed by the development of an algorithm to decompose, and solve each problem distributedly. The binary (UE association) and continuous (power, deployment) variables are separated using the Bender decomposition (BD), and then the Dinkelbach algorithm (DA) is used to convert fractional programming into an equivalent solvable form in the subproblem. A standard optimization solver is utilized to deal with the complexity of the master problem for binary variables. The alternating direction method of multipliers (ADMM) algorithm is used to solve the subproblem for the continuous variables. Our proposed algorithm provides a suboptimal solution, and simulation results demonstrate that the proposed algorithm achieves better EE than baselines.

Index Terms—Sixth-generation networking, space-air-sea communication, satellite-access networks, unmanned aerial vehicle, Bender decomposition, Dinkelbach algorithm, alternating direction method of multipliers.

I. INTRODUCTION

Research on 6G wireless networks is currently underway in both academia and industry [1]. One major component of 6G networks is non-terrestrial networks (NTNs) that consist of space and aerial-based networking [2]. NTNs are expected to provide global connectivity to regions and areas that are out of reach of existing terrestrial networks. For instance, NTNs can provide wireless network access to maritime users, called

low-end user equipment (UE), that cannot directly connect to any satellite. In particular, these low-end UEs can get network services from an aerial access network near them [3]. However, high-end UEs can directly connect with low-earth orbit (LEO) satellites. Thus, a coordinated space-air-sea (SAS)-based NTN network can extend the existing coastline base stations (CBSs) coverage seamlessly. This heterogeneous SAS-NTN can meet the increasing maritime network requirements, i.e., seamless, energy-efficient, and high throughput coverage. The design of NTNs faces many challenges, including the coordinated integration of space, air, and sea platforms. While some of these issues have been addressed in the past (see Section II), nonetheless, the joint maritime users' fronthaul and backhaul communication mechanisms and UAV deployment techniques in heterogeneous networks are missing.

The main contribution of this paper is a novel SAS-NTNs architecture that enabled each maritime UE to connect with the terrestrial networks. For reliable communication in this network, maritime users with a high gain antenna, i.e., high-end UEs (HUEs), can directly associate with a LEO satellite or a CBS depending on their vicinity. However, low-end UEs (LUEs) cannot effectively communicate with a LEO satellite or a CBS due to low antenna gain [4]. In particular, LUEs require assistance from UAVs, i.e., UAVs could transmit LUEs' data to a LEO satellite or CBS, using aerial-to-satellite (A2S) links [5] or aerial-to-ground (A2G) links. These LUEs limit themselves for long transmission distance due to power consumption constraints [6]. As a result, the UAV is regarded as an effective mode of communication for LUEs in the maritime environment. UAVs are quickly deployed on the place of interest, which is critical in isolated maritime regions [7]. Our key contributions are summarized as follows:

- We propose a novel heterogeneous SAS network architecture for next-generation maritime mobile networks. To serve maritime users, we propose the use of a LEO satellite coupled with UAVs and CBSs for the service provisioning of low-end and high-end UEs.
- We study the problem of resource management in the SAS-NTNs to optimize resource block allocation, transmit power control, and UAVs deployment for maximizing network energy efficiency (EE). An energy efficiency maximization problem is formulated by considering the constraint of the limited payload of UAVs and also their power consumption.

Sheikh Salman Hassan, Do Hyeon Kim, Yan Kyaw Tun, and Choong Seon Hong are with the Department of Computer Science and Engineering, Kyung Hee University, Yongin-si, Gyeonggi-do 17104, Rep. of Korea, e-mails: {salman0335, doma, ykyawtun7, cshong}@khu.ac.kr.

Nguyen H. Tran is with the School of Computer Science, The University of Sydney, Sydney, NSW 2006, Australia (e-mail: nguyen.tran@sydney.edu.au).

Walid Saad is with the Bradley Department of Electrical and Computer Engineering, Virginia Tech, VA, 24061, USA, and the Department of Computer Science and Engineering, Kyung Hee University, Yongin-si, Gyeonggi-do 17104, Rep. of Korea, email: {walids@vt.edu}.

- The problem of resource allocation in the SAS maritime network is formulated as a mixed-integer nonlinear programming (MINLP) problem. The goal is to optimize the utility function considering the energy efficiency of the network.
- Due to the problem's high complexity, we propose a novel algorithm to solve the MINLP problem, composed of the Bender's decomposition (BD), Dinkelbach algorithm (DA), alternating direction method of multipliers (ADMM) algorithm, and an optimization solver.
- The BD algorithm decomposes the main problem into a master problem and another subproblem to obtain the solution efficiently. The variables of the original problem are divided into two subsets so that a first-stage master problem is solved over the first set of variables, and the values for the second set of variables are determined in a second-stage subproblem for a given first-stage solution.
- We use the Dinkelbach algorithm for the subproblem to transform fractional programming into an equivalent form and adopt ADMM in the inner loop to distributedly solve the continuous large-scale problem. We use the optimization solver in the master problem to solve pure integer programming with complexity reduction considerations.
- We evaluate the performance of our proposed algorithm in the simulation. Our numerical results demonstrate that the proposed algorithm achieves a near-optimal solution and outperforms the other baselines. The proposed algorithm achieves EE up to 9% and 10% compared to greedy and dynamic algorithms, respectively.

The rest of this paper is organized as follows. In Section II, the research background and the objective are presented. Section III represents the system model. In Section IV, we formulate the optimization problem. In Section V, the problem decomposition and the proposed algorithms are presented. Numerical results and corresponding analyses are provided in Section VII. The main notations are given in Table I.

II. RELATED WORK

We now review the prior works in the area of NTN, satellite and UAV-based networking, maritime communication, and their combinations. We particularly show the classification of maritime users, i.e., we can provide networking resources to each maritime user based on their antenna gain and feasible connectivity. Despite significant advances, prior works remain limited as they do not address the challenges of maritime users' resource allocation based on their classification and overall network energy efficiency by jointly considering all the network nodes involved in SAS-NTNs.

Various elements of NTNs such as LEO satellite constellation deployment have been examined in the literature, including satellite number minimization [8] and [9], coverage maximization [10], communication latency reduction [11], and heterogeneous network design [12]. For satellite constellation optimization, several intelligence algorithms are used, including the genetic algorithm (GA), differential evolution (DE),

immune algorithm, and particle swarm optimization (PSO) [24]. The work in [9] developed a non-dominated sorting evolutionary algorithm for regional LEO satellite constellation design to match UE needs while reducing satellite cost. The authors in [13] proposed a satellite constellation for continuous mutual regional coverage based on the evolutionary optimization approach. It has been explored the relationship between the coverage ratio and the number of satellites. The works in [10] and [14] used an evolutionary algorithm to optimize the coverage of target areas while designing regional satellite constellations. To reduce the end-to-end latency, authors in [11] devised a progressive satellite constellation network building method. The work in [15] investigated the use of LEO satellites within the context of the Internet of Things. The performance of satellite constellation design with a few intelligent algorithms, i.e., GA, DE, immunity algorithm, and PSO, was compared in [16] to enhance satellite coverage capabilities. NTNs face a slew of new difficulties, including high bit error rates, extended propagation delays, and unreliable connections. As a result, it's important to think about how to incorporate network operations into NTNs efficiently.

A significant number of related prior works on NTNs focused on solutions that can improve the connectivity of ground networks by using UAVs [17]–[32]. The authors in [17]–[29] concentrate primarily on static type UEs. The authors in [30]–[32] investigated how to optimize the ergodic achievable rate by remotely monitoring the UAV trajectory to deal with the moving UEs. Meanwhile, the rotary-wing UAV placement problem is widely studied to provide useful results. However, in the case of fixed wing UAVs, the key issue is their optimum transmission and trajectory. In particular, the trajectory of UAVs is determined by taking into account the maximum velocity or acceleration to achieve the maximum sum rate, the minimum service flight time, and the optimum energy efficiency in the network.

There have been a number of recent works that looked at the co-existence of UAVs and ground base stations (GBSs) [33]–[37]. The use of a GBS as a central controller for a UAV-based network was proposed in [33] to maximize the sum rate by taking radio access and backhaul links into account. To counter the dynamics of UAV-based networks, the authors in [34] proposed the idea of multihop backhaul networks. The works in [35]–[37] analyzed the outage probability of the GBS and UAV networks. In [37], the authors studied the sum rate of the network by taking outage probability into account. The authors in [38] studied a GBS and multiple offshore relay nodes for a cooperative multicast communication strategy for maritime users based on combined beamforming (BF) optimization and relay design. The authors in [39] provide a maritime communication network design in which a GBS provides wireless backhaul for shipborne base stations, while the shipborne base stations act as mobile access points for user ships. Although GBS may provide end-users with real-time services and high data rates, their network coverage in marine communication is restricted. Furthermore, deploying expensive floating edge computer equipment in deep oceans is too expensive. Consider UAV technology, which necessitates the use of edge servers to deliver seamless and real-time

services to moving boats. An edge server's coverage diameter (e.g., a tiny cell base station) is often less than 300 m. As a result, moving vessels will encounter frequent handovers in GBS networks. More critically, vessels engaged in marine communication may lose network connectivity.

In addition, several recent works [40]–[45] studied the use of multi-layer heterogeneous network architectures for NTN. Specifically, in [42], the authors studied the problem of UAV satellite integration for a hybrid flying autonomous vehicle. Meanwhile, the authors in [43] investigated the optimal altitude of UAV to analyze the suitable coordination in case of communication between satellite and UAV with a focus on reducing latency. Similarly, the work in [44] analyzed the coverage and rate of a multi-UAV network in a disaster scenario. In [45], the authors considered an airborne cellular network and studied the problem of resource allocation, i.e., transmit power control for the various time-critical application.

In this prior art [33]–[37], [40]–[45], the spectrum resources that have a direct effect on the EE of a SAS-NTN were not taken into account. To examine the relationship between the satellite backhaul, the CBS backhaul links, and the radio access linkages in SAS networks, it is essential to consider the joint problem of user association, resource allocation across all communication links within the SAS network, and the deployment of UAVs above sea region which is missing in the literature. However, the preceding studies all regarded satellites, UAVs, and CBS to be the only network node of SAS-NTNs. Furthermore, prior works primarily consider direct connections, leaving out backhaul transmission. In response to the aforementioned finding, we offer a unique SAS-NTNs architecture to overcome the maritime UEs communication problem according to their classification. For SAS-NTNs EE, a combined problem of UE association, power control, and UAV deployment is developed.

III. SYSTEM MODEL

As shown in Fig. 1, we consider a realistic heterogeneous SAS maritime communication network consisting of a LEO satellite¹ s , a set \mathcal{U} of U UAVs that serve as aerial base stations (ABSs)², and a set \mathcal{C} of C CBSs. The coverage area of each CBS is planar in the sea with a radius ν centered at $(0, 0) \in \mathbb{R}^2$. We define a set \mathcal{M}_l of M_l LUEs and a set \mathcal{M}_h of M_h HUEs. We define a set $\mathcal{M} = \mathcal{M}_l \cup \mathcal{M}_h$ of M maritime UEs. To capture the dynamic nature of the nodes, i.e., satellite, ABSs, and UEs. We consider the network within a certain time duration T that is divided into a set \mathcal{N} of $N - 1$ time slots. Due to the short duration in each time slot n , the network configuration is considered fixed. Therefore, we will then analyze network performance in a one-time slot. CBS can serve the coastal region, but its broadband services are limited due to significant non-line-of-sight path loss. Various UEs are present in the waters, such as cruise ships and vessels equipped with high gain antennas that can directly connect with the

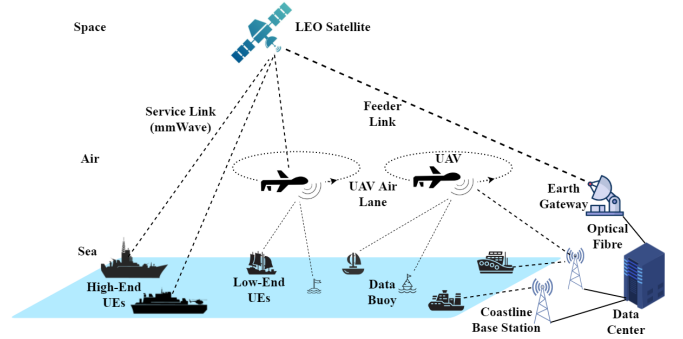


Figure 1: Illustration of space-air-sea networks architecture.

satellite or a CBS depending upon their location. Conversely, LUEs, e.g., seamen, fishers, offshore platform users, maritime internet-of-things (MIoT) devices within the coverage region of the satellite or CBSs, cannot directly access their services and require service by ABSs. However, the satellite and CBSs will provide radio access to the HUEs and backhaul services to the deployed ABSs.

A. Communication Model

In the considered scenario, all the communication links operate over the Ka-band (26.5 – 40 GHz), which is a well-defined millimeter wave (mmW) range suitable for satellite communication and future 5G links, as discussed in [46]. Directional transmissions over the mmW band are unavoidable to resolve the incredibly high path loss. Consequently, in compliance with established standards such as IEEE 802.15.3c [47], a service provider node uses the multi-access time division scheme (TDMA) to provide services to its maritime users. Each maritime UE is a set element that seeks services that must be scheduled over the mmW band at each time slot n . In practice, the mmW transceiver must align its beams during a beam training stage so that the maximum beamforming gain is achieved. This phase of training will introduce a non-negligible TDMA system overhead, which can be particularly important as the number of mmW users increases. We assume that a beam training overhead time per transmission over the mmW band had already been established for the training phase as given in [47]. Moreover, due to the considerable distance between the satellite and LUEs, the interference experienced by LUEs from the satellite is negligible. Although each ABS shares the same frequency spectrum to provide downlink services to LUEs, therefore these LUEs experience interference from non-associated ABSs. Similarly, the satellite and CBSs share the same frequency spectrum, which also leads to interference at the ABSs and HUEs.

B. Network Deployment Model

The satellite orbits at an altitude h_s (from the sea surface), and it provides wireless backhaul connectivity to ABSs and radio access to HUEs in its coverage region. The ABSs are

¹Hereinafter, the satellite is considered as a LEO satellite unless otherwise stated.

²Hereinafter, the UAV is considered as an ABS unless otherwise stated.

sparingly deployed on the sea near coastal areas [48] to provide connectivity to the set of LUEs in their coverage region. This model considers that each ABS has a total mission flight time T . During T , each ABS u must serve LUEs in its coverage region. As mentioned earlier, the UAV flight time T is discretized into a set \mathcal{N} of N equally-spaced time slots with the length of each time slot is given as $L_u = \frac{T}{N}$. Moreover, the value of N should be properly chosen to guarantee that the ABS location remains unchanged within each time slot and fulfill the network requirements, i.e., task processing. Each ABS u flies at a fixed height h_u above the sea surface in each time slot n . Thus, at each slot n , the position of each ABS u in three-dimensional coordinates will be:

$$\mathbf{d}_u(n) = \left[(x_u(n), y_u(n), h_u) \right]^T, \forall u \in \mathcal{U}, \forall n \in \mathcal{N}. \quad (1)$$

Similarly, the position of an LUE m_l is $\mathbf{d}_{m_l} = (x_{m_l}(n), y_{m_l}(n), 0)$, and the position of a HUE m_h will be $\mathbf{d}_{m_h} = (x_{m_h}(n), y_{m_h}(n), 0)$. Both types of UEs will be distributed in a specified region at sea. Moreover, the position of each CBS can be represented by $\mathbf{d}_c = (x_c, y_c, 0)$. Additionally, the satellite position can be given by $\mathbf{d}_s = (x_s, y_s, h_s)$, which remains constant during the studied time. The ABS backhaul service can be provided by the satellite, or a CBS [49] depends upon its position in each time slot n .

C. ABS Energy Consumption Model

The ABS's overall energy consumption is made up of two parts. The first is an energy associated with communications, and this energy is generated by radiation, signal processing, and other electronics. The other component of energy is propulsion, which is required to keep the UAV aloft as well as to support its movement if necessary. We consider an autonomous ABS that can operate as an aerial relay node and a base station in a sea environment. This ABS can perform resource allocation, dynamic mission planning, inter-cell handover, and other tasks [50]. The maximum speed of the ABS in each time slot is v_{\max} . Thus, the maximum distance that an ABS travels within each time slot will be $L_u v_{\max}$. The energy consumption of the ABS for traveling from one location to another in each time slot can be given by [51]:

$$E_u^{\text{flight}}(n) = \left(\kappa_u \|v_u(n)\|^3 + \frac{\zeta_u}{\|v_u(n)\|} + \frac{\zeta_u \|\mu_u(n)\|^2}{q^2 \|v_u(n)\|} \right) + \frac{\Delta J}{\Lambda}, \forall u \in \mathcal{U}, \quad (2)$$

where κ_u and ζ_u are constants which depends on the ABS characteristics (e.g., weight, wing size, air density, etc.), Λ is any infinitesimal time step, q is the gravitational acceleration, and $\Delta J = \frac{1}{2}\pi (\|v_n(n+1)\|^2 - \|v_n(n)\|^2)$ is the kinetic energy. Here, π is the mass of the UAV's payload³, v_u is the speed, and μ_u is the acceleration of each ABS n . We assume that the distance of each ABS to UEs, CBSs, and the satellite remains constant within each time slot n . The operating time of each ABS u is calculated primarily by the fuel for flying and the battery for communication. The fuel of a

³Hereinafter, we ignore the change in weight of the ABS as more battery and fuel are consumed over time for simplicity.

Table I: SUMMARY OF NOTATIONS

Notation	Description
\mathbf{d}_u	3D coordinates of ABS $u \rightarrow \mathbf{d}_u = \{x_u, y_u, h_u\}$
\mathbf{d}_{m_l}	Position of low-end UEs $m_l \rightarrow \mathbf{d}_{m_l} = \{x_{m_l}, y_{m_l}, 0\}$
\mathbf{d}_{m_h}	Position of high-end UEs $m_h \rightarrow \mathbf{d}_{m_h} = \{x_{m_h}, y_{m_h}(n), 0\}$
$\mathbf{d}_s(n)$	Position of the satellite $s \rightarrow \mathbf{d}_s = \{x_s, y_s, h_s\}$
\mathbf{d}_c	Position of the CBS $c \rightarrow \mathbf{d}_c = \{x_c, y_c, 0\}$
K_u	Set of resource blocks allocated for each ABS u
Z_s	Set of resource blocks allocated for a LEO satellite
Y_c	Set of resource blocks allocated for each CBS
g_{u,m_l}	Radio-access channel gain from ABS u to low-end UE m_l
$g_{s,u}$	Backhaul channel gain from satellite s to ABS u
$g_{c,u}$	Backhaul channel gain from CBS c to ABS u
g_{s,m_h}	Radio-access channel gain from satellite s to high-end UE m_h
g_{c,m_h}	Radio-access channel gain from CBS c to high-end UE m_h
p_{u,m_l}	Transmit power from ABS u to low-end UE m_l
$p_{s,u}$	Transmit power from satellite s to ABS u
$p_{c,u}$	Transmit power from UAV u relay node to CBS c
p_{s,m_h}	Transmit power from satellite s to ABS u
p_{c,m_h}	Transmit power from CBS c to ABS u
γ_{u,m_l}	SNR between ABS u and low-end UE m_l
$\gamma_{s,u}$	SNR between satellite s and ABS u
$\gamma_{c,u}$	SNR between CBS c and ABS u
γ_{s,m_h}	SNR between satellite s and high-end UE m_h
γ_{c,m_h}	SNR between CBS c and high-end UE m_h
$r_{m_l,u}$	Achievable datarate from ABS u to low-end UE m_l
$r_{s,u}$	Achievable datarate from satellite s to ABS u
$r_{c,u}$	Achievable datarate from CBS c to ABS u
r_{s,m_h}	Achievable datarate from satellite s to high-end UEs m_h
r_{c,m_h}	Achievable datarate from CBS c to high-end UEs m_h

fixed-wing ABS is assumed to be large enough for our studied time of the network performance. To validate the obtained energy consumption model, we investigate the case of steady, straight and fixed heights with constant speed V , i.e., $v(n) = V$ and $\mu_u(n) = 0$. Then, (2) can be modified as:

$$E_u^{\text{flight}}(n) = (\kappa_u V^3 + \frac{\zeta_u}{V}). \quad (3)$$

Equation (3) is a classical model of the energy consumption in aerodynamics [52]. The model comprises two components in (3), where V^3 is used to overcome the parasite drag and $\frac{1}{V}$ allows overcoming the elevated drag. Therefore, the flying ABSs power can be calculated as:

$$P_u^{\text{flight}}(n) = E_u^{\text{flight}}(n) \times L_u, \quad (4)$$

where L_u represents the duration of each time step.

D. Low-End UE-ABS Data Link Analysis

In the SAS network, each ABS u is placed at a high-enough altitude to enable LoS transmission. Therefore, we use a general composite channel model coefficient that consists of both small-scale and large-scale fading between each ABS u and the low-end UE m_l at each time slot n , as follows:

$$g_{u,m_l}(n) = \beta_{u,m_l}(n) \sqrt{\xi_{u,m_l}(n)}, \quad (5)$$

where $\beta_{u,m_l}(n)$ is the small-scale fading coefficient with $\mathbb{E}[|\beta_{u,m_l}|^2] = 1.53$ [53] and $\xi_{u,m_l}(n)$ is the large-scale fading coefficient. Each ABS knows the coordinates of LUEs and

channel distribution information, i.e., ξ_o and $|\beta_{u,m_l}|^2$. The large scale fading at each time slot n will be:

$$\xi_{u,m_l}(n) = \frac{\xi_o}{\|(\mathbf{d}_u(n) - \mathbf{d}_{m_l}(n))\|^2}, \forall u \in \mathcal{U}, m_l \in \mathcal{M}_l, n \in \mathcal{N}. \quad (6)$$

In (6), ξ_o is the reference channel gain at 1m and $\|(\mathbf{d}_u - \mathbf{d}_{m_l})\|^2$ is 3D Euclidean distance between ABS u and low-end UE m_l . We consider a Rician distribution for modeling the small-scale fading between LUE m_l and ABS u to compensate for the LoS and multipath scatterers that can be experienced by each receiving LUE in the network. Specifically, adopting the Rician channel model is justified by the fact that the channel between ABS u and LUE m_l is primarily dominated by LoS [54]. Moreover, the Doppler effect due to mobility in network nodes is compensated by existing frequency synchronization techniques, i.e., phase-locked loop as discussed in [55]–[57]. Each ABS shares the same set of resource blocks to provide downlink services to LUEs. Therefore, the interference in ABS-LUE link from non-associated ABSs and CBSs at time slot n will be $\Omega_{u,m_l} = \sum_{\forall u' \neq u} \sum_{\forall m_l' \neq m_l} p_{u'} g_{u',m_l'} + \sum_{\forall c \in \mathcal{C}} p_c g_{c,m_l}$. Here u' is non-associated ABSs, $p_{u'}$ is the transmit power of non-associate ABSs, and p_c is the transmit power of CBSs. Thus, the signal-to-noise ratio (SINR) between this link can be given as:

$$\gamma_{u,m_l}(n) = \frac{p_{u,m_l}(n)g_{u,m_l}(n)}{\Omega_{u,m_l} + \sigma^2}, \quad \forall u \in \mathcal{U}, m_l \in \mathcal{M}_l, n \in \mathcal{N}, \quad (7)$$

where $p_{u,m_l}(n)$ is the transmit power of ABS u to low-end UE m_l in the k th RB, and σ^2 is the the noise power. Moreover, following [58], even when there is additional interference at the receiver, we suppose that the aggregate interference follows a Gaussian distribution and the corresponding power is incorporated into the noise term σ^2 . The achievable data rate without transmission diversity between low-end UE m_l and ABS u in each time slot n will be:

$$r_{u,m_l}(n) = B_u \log_2 (1 + \gamma_{u,m_l}(n)), \quad (8)$$

where B_u is the bandwidth of each RB k over the band allocated from ABS u to LUEs m_l at time slot n .

E. Satellite based ABS Backhaul Link Analysis

The satellite provides backhaul services to the ABSs outside of the CBS coverage region. Therefore, we consider that the ABS u and the satellite s are equipped with one antenna each. Therefore, the channel model between ABS u and the satellite s can be define as:

$$g_{s,u}(n) = \beta_{s,u}(\xi_{s,u})^{-1/2}, \quad \forall u \in \mathcal{U}, n \in \mathcal{N}. \quad (9)$$

where $\beta_{s,u}$ is the Rician fading channel coefficient and $\xi_{s,u}$ represents large-scale fading for pathloss. The $d_{s,u} = \left(\sqrt{(x_s - x_u)^2 + (y_s - y_u)^2 + (z_s - z_u)^2}\right)$ denotes the distance between satellite s and ABS u . Thus, large-scale path loss on the mmW links will be given by [59]:

$$\xi_{s,u}(\text{dB}) = \omega_{s,u} + \zeta_{s,u} 10 \log_{10} \left(\frac{d_{s,u}(n)}{d_0} \right) + \psi_{s,u} \quad (10)$$

where $\zeta_{s,u}$ is the slope of the fit (path loss exponent), $\omega_{s,u}$ indicate the intercept parameter (path loss at reference distance d_0) [47], and $\psi_{s,u}$ models the deviation in fitting (dB) which is a zero mean Gaussian random variable with standard deviation δ_u . The small scale fading coefficient will be:

$$\beta_{s,u} = \sqrt{\frac{K_{s,u}}{1 + K_{s,u}}} + \sqrt{\frac{1}{1 + K_{s,u}}} \Xi_{s,u}, \quad (11)$$

where $K_{s,u}$ is the Rician factor and $\Xi_{s,u} \sim \mathcal{N}(0, 1)$. We can now simplify the channel gain:

$$g_{s,u}(n) = \left(\frac{d_0}{d_{s,u}(n)} \right)^{\frac{\zeta_{s,u}}{2}} 10^{-\frac{\omega_{s,u} + \psi_{s,u}}{20}} \left(\sqrt{\frac{K_{s,u}}{1 + K_{s,u}}} + \sqrt{\frac{1}{1 + K_{s,u}}} \Xi_{s,u} \right) \quad (12)$$

The interference at time slot n in this link from CBSs will be $\Omega_{s,u} = \sum_{\forall c \in \mathcal{C}} p_c g_{c,u}$. Here p_c is the transmit power of CBSs.

Thus, the SINR between this link can be given as:

$$\gamma_{s,u}(n) = \frac{p_{s,u}(n)g_{s,u}(n)}{\Omega_{s,u} + \sigma^2}, \quad \forall u \in \mathcal{U}, \forall n \in \mathcal{N}, \quad (13)$$

where $p_{s,u}(n)$ is the transmit of satellite s in the z th RB to ABS u at time slot n . The achievable data rate between satellite s and ABS u in each time slot n can be calculated by Shannon capacity:

$$r_{s,u}(n) = B_s \log_2 (1 + \gamma_{s,u}(n)), \quad (14)$$

where B_s denotes the bandwidth allocated to the channel from satellite s to UAV u at time slot n .

F. CBS based ABS Backhaul Link Analysis

The CBS provides backhaul services to the ABSs near coastline under their coverage region. Therefore, the channel model between ABS u and the CBS c will be:

$$g_{c,u}(n) = \beta_{c,u}(\xi_{c,u})^{-1/2}, \quad \forall c \in \mathcal{C}, u \in \mathcal{U}, n \in \mathcal{N}, \quad (15)$$

where $\beta_{c,u}$ is the Rician fading channel coefficient and $\xi_{c,u}$ represents the large-scale fading. $d_{c,u} = \left(\sqrt{(x_c - x_u)^2 + (y_c - y_u)^2 + (z_c - z_u)^2}\right)$ is the distance between CBS c and ABS u . Thus, large-scale path loss on the mmW links will be:

$$\xi_{c,u}(\text{dB}) = \omega_{c,u} + \zeta_{c,u} 10 \log_{10} \left(\frac{d_{c,u}(n)}{d_0} \right) + \psi_{c,u}, \quad (16)$$

where $\zeta_{c,u}$ is the slope of the fit (path loss exponent), $\omega_{c,u}$ is the intercept parameter (path loss at reference distance d_0) [47], and $\psi_{c,u}$ models the deviation in fitting (dB) which is a zero mean Gaussian random variable with standard deviation δ_c . The small scale fading coefficient will be:

$$\beta_{c,u} = \sqrt{\frac{K_{c,u}}{1 + K_{c,u}}} + \sqrt{\frac{1}{1 + K_{c,u}}} \Xi_{c,u}, \quad (17)$$

where $K_{c,u}$ is the Rician factor and $\Xi_{c,u} \sim \mathcal{N}(0, 1)$. We can then simplify the channel gain:

$$g_{c,u}(n) = \left(\frac{d_0}{d_{c,u}(n)} \right)^{\frac{\zeta_{c,u}}{2}} 10^{-\frac{\omega_{c,u} + \psi_{c,u}}{20}} \left(\sqrt{\frac{K_{c,u}}{1 + K_{c,u}}} + \sqrt{\frac{1}{1 + K_{c,u}}} \Xi_{c,u} \right). \quad (18)$$

The interference at time slot n in this link from non-associated CBSs will be $\Omega_{c,u} = \sum_{\forall c' \neq c} p_{c'} g_{c',u}$. Here c' is non-associated CBSs, and $p_{c'}$ is the transmit power of non-associated CBSs. Thus, the SINR between this link can be given as:

$$\gamma_{c,u}(n) = \frac{p_{c,u}(n)g_{c,u}(n)}{\Omega_{c,u} + \sigma^2}, \forall c \in \mathcal{C}, \forall u \in \mathcal{U}, \forall n \in \mathcal{N}, \quad (19)$$

where $p_{c,u}(n)$ is the transmit of CBS c to ABS u over the y th RB at time slot n . The achievable data rate between CBS c and ABS u in each time slot n can be calculated by Shannon capacity:

$$r_{c,u}(n) = B_c \log_2 (1 + \gamma_{c,u}(n)), \quad (20)$$

where B_c is the bandwidth allocated to the channel from CBS c to ABS u at time slot n .

G. Satellite-HUEs Data Link Analysis

In the SAS network, HUEs are considered with a high gain antenna that can directly connect with the satellite s . The satellite provides backhaul services to HUEs out of the CBS coverage region. Therefore, we consider that the satellite s and the HUE m_h are equipped with one antenna. Therefore, the channel model between the satellite s and HUE m_h will be:

$$g_{s,m_h}(n) = \beta_{s,m_h} (\xi_{s,m_h})^{-1/2}, \quad \forall m_h \in \mathcal{M}_h, \forall n \in \mathcal{N}, \quad (21)$$

where β_{s,m_h} is the Rician fading channel coefficient and ξ_{s,m_h} represents the large-scale fading for pathloss. $d_{s,u} = \left(\sqrt{(x_s - x_u)^2 + (y_s - y_u)^2 + (z_s - z_u)^2} \right)$ is the distance between satellite s and HUE m_h . Thus, the large-scale path loss on the mmW link will be [59]:

$$\xi_{s,m_h}(\text{dB}) = \omega_{s,m_h} + \zeta_{s,m_h} 10 \log_{10} \left(\frac{d_{s,m_h}(n)}{d_0} \right) + \psi_{s,m_h} \quad (22)$$

where ζ_{s,m_h} is the slope of the fit (path loss exponent), ω_{s,m_h} indicate the intercept parameter (path loss at reference distance d_0) [47], and ψ_{s,m_h} models the deviation in fitting (dB) which is a zero mean Gaussian random variable with standard deviation δ_{m_h} . The small scale fading coefficient will be:

$$\beta_{s,m_h} = \sqrt{\frac{K_{s,m_h}}{1 + K_{s,m_h}}} + \sqrt{\frac{1}{1 + K_{s,m_h}}} \Xi_{s,m_h}, \quad (23)$$

where K_{s,m_h} is the Rician factor and $\Xi_{s,m_h} \sim \mathcal{N}(0, 1)$. We can then simplify the channel gain:

$$g_{s,m_h}(n) = \left(\frac{d_0}{d_{s,m_h}(n)} \right)^{\frac{\zeta_{s,m_h}}{2}} 10^{-\frac{\omega_{s,m_h} + \psi_{s,m_h}}{20}} \left(\sqrt{\frac{K_{s,m_h}}{1 + K_{s,m_h}}} + \sqrt{\frac{1}{1 + K_{s,m_h}}} \Xi_{s,m_h} \right) \quad (24)$$

The interference at time slot n in this link from non-associated ABSs and CBSs will be $\Omega_{s,m_h} = \sum_{\forall u \in \mathcal{U}} p_u g_{u,m_h} + \sum_{\forall c \in \mathcal{C}} p_c g_{c,m_h}$. Here p_u is the transmit power of ABS u and p_c is the transmit power of CBS c . Thus, the SINR between this link can be given as:

$$\gamma_{s,m_h}(n) = \frac{p_{s,m_h}(n)g_{s,m_h}(n)}{\Omega_{s,m_h} + \sigma^2}, \quad \forall m_h \in \mathcal{M}_h, \forall n \in \mathcal{N}, \quad (25)$$

where p_{s,m_h} is the transmit of satellite s to HUE m_h over the z th RB at time slot n . The achievable data rate between satellite s and HUE m_h in each time slot n can be calculated by Shannon capacity:

$$r_{s,m_h}(n) = B_s \log_2 (1 + \gamma_{s,m_h}(n)), \quad (26)$$

where B_{m_h} is the bandwidth allocated to the channel from satellite s to HUE m_h at time slot n .

H. CBS-HUEs Data Link Analysis

Each CBS provides backhaul services to the HUEs near the coastline under their coverage region. Although empirical path loss models can accurately forecast average signal intensity in the marine environment, they are unable to account for the local oscillations caused by the destructive summing of sparse multipath signals. Ray trajectory-based path loss models mathematically detect the trajectories of the most dominating rays arriving at the receiver to solve this problem. As a result, the phase shift of each ray is described and taken into account in the path loss computation, resulting in a more accurate representation of the received signal strength's local peaks and nulls [60]. Therefore, path loss between a CBS c and a HUE m_h link can be modeled as curved-earth two-ray (CE2R) which take into account the earth curvature [60]:

$$\xi_{c,m_h} = -10 \log_{10} \left\{ \left(\frac{\lambda}{4\pi d_{c,m_h}} \right)^2 \left[2 \sin \left(\frac{2\pi h_c h_{m_h}}{\lambda d_{c,m_h}} \right) \right]^2 \right\},$$

where ξ_{c,m_h} is the propagation loss in dB, λ indicate wavelength of signal, h_c and h_{m_h} is the height of CBS c and HUE m_h , respectively. Additionally, $d_{c,m_h}(n)$ is the 3D Euclidean distance between CBS c and HUE m_h at each time slot n as:

$$d_{c,m_h}(n) = \| (\mathbf{d}_c(n) - \mathbf{d}_{m_h}(n)) \|^2, \forall c \in \mathcal{C}, \forall m_h \in \mathcal{M}_h, \forall n \in \mathcal{N}, \quad (27)$$

The channel gain between this link can be given as:

$$g_{c,m_h}(n) = \beta_{c,m_h} 10^{-\xi_{c,m_h}(n)/10}, \quad \forall c \in \mathcal{C}, u \in \mathcal{U}, n \in \mathcal{N}. \quad (28)$$

The interference at time slot n in this link from ABSs and non-associated CBSs will be $\Omega_{c,m_h} = \sum_{\forall u \in \mathcal{U}} p_u g_{u,m_h} + \sum_{\forall c' \neq c} \sum_{\forall m'_h \neq m_h} p_{c'} g_{c',m'_h}$. Here c' is non-associated CBSs, $p_{c'}$ is the transmit power of non-associate CBSs, and p_u is the transmit power of ABSs. Thus, the SINR between this link will be:

$$\gamma_{c,m_h}(n) = \frac{p_{c,m_h}(n)g_{c,m_h}(n)}{\Omega_{c,m_h} + \sigma^2}, \quad \forall c \in \mathcal{C}, m_h \in \mathcal{M}_h, n \in \mathcal{N}, \quad (29)$$

where $p_{c,m_h}(n)$ is the transmit of CBS's c to HUE over y th RB at time slot n . The achievable data rate between CBS c and high-end UE m_h in each time slot n can be calculated by Shannon capacity:

$$r_{c,m_h}(n) = B_c \log_2 (1 + \gamma_{c,m_h}(n)), \quad (30)$$

where B_c is the bandwidth allocated to the channel from CBS c to HUE m_h at time slot n .

IV. TOWARDS AN ENERGY-EFFICIENT HETEROGENEOUS SAS-NTN MARITIME NETWORKS

Our main objective is to provide a decentralized approach that enables the network operator to manage each marine UE and to find its optimal resource allocation based on both its position and user type. Therefore, we seek to maximize the network energy efficiency η by factoring in the sum rate R_t and total power P_t . Moreover, we need to find the optimal 3D coordinates of the ABSs \mathbf{d}_u . To realize this, we optimize the position of the ABSs jointly with the marine UEs association \mathbf{a} and transmit power control \mathbf{p} . We formulate the resource allocation and ABSs deployment problem of maximizing the system energy efficiency (Bit/Joule) for the SAS-NTN networks. To formulate this problem, we next define a series of constraints as follows:

Each ABS must return to its initial position at the end of the flight time. This constraint ensures downlink connectivity to LUEs in the marine environment with the pre-defined route and stationary points, so each ABS must travel within the specified area [48]:

$$\mathbf{d}_u(1) = \mathbf{d}_u(N), \quad \forall u \in \mathcal{U}. \quad (31)$$

Then we have the following constraint, which ensures that the distance covered by the ABS between two consecutive time slots corresponds to the distance that can be calculated by the speed and time limits. The ABS's mobility is restricted by its maximum propulsion speed, v_{\max} . Furthermore, ABS requires a minimum stall speed v_{\min} in some severe conditions to retain mobility.

$$\|\mathbf{d}_u[n+1] - \mathbf{d}_u[n]\| \leq (v_{\max}L_u), \quad \forall u \in \mathcal{U}, \forall n \in \mathcal{N}. \quad (32)$$

To ensure the kinematic energy budget for each ABS, the threshold must be met at each time slot n of the flight:

$$E_u^{\text{flight}}(n) \geq E_{\text{th}}(n), \quad \forall u \in \mathcal{U}, \forall n \in \mathcal{N}. \quad (33)$$

The ABS's flight power consumption should be:

$$P^{\text{flight}}(n) \geq \frac{E_u^{\text{flight}}(n)}{L_u}, \quad \forall u \in \mathcal{U}, \forall n \in \mathcal{N}. \quad (34)$$

The flight speed of each ABS should be within the range at which the LUEs downlink criterion must be met:

$$v_{\min}(n) \leq v_u(n) \leq v_{\max}(n), \quad \forall u \in \mathcal{U}, \forall n \in \mathcal{N}, \quad (35)$$

where $v_{\min}(n)$ and $v_{\max}(n)$ denote the minimum and maximum speed of each ABS at the time slot n respectively. The ABS speed limit can be adjusted according to the LUEs requirements [61]. The boundary conditions for each ABS altitude to ensure LoS connections for LUEs have also been established:

$$h_{\min}(n) \leq h_u(n) \leq h_{\max}(n), \quad \forall u \in \mathcal{U}, \forall n \in \mathcal{N}, \quad (36)$$

where h_{\min} ensures a LoS link between the ABS and LUEs, and h_{\max} is an upper bound defined by air traffic control [62]. It is considered that each ABS can utilize the satellite (space-to-air) or any CBS (coastline-to-air) for backhaul connectivity. The aggregated achievable rate of all ABSs-to-LUEs links

should remain within the channel capacity of satellite-to-ABS and CBS-to-ABS links. These constraints guarantee the capacity of the backhaul as follows:

$$\sum_{u=1}^U \sum_{m_l=1}^{M_l} r_{u,m_l}(n) \leq \sum_{u=1}^U r_{u,s}(n), \quad \forall n \in \mathcal{N}, \quad (37)$$

$$\sum_{u=1}^U \sum_{m_l=1}^{M_l} r_{u,m_l}(n) \leq \sum_{c=1}^C \sum_{u=1}^U r_{c,u}(n), \quad \forall n \in \mathcal{N}. \quad (38)$$

Each ABS u need to satisfy the demand of each associated LUEs data rate which can be defined as:

$$\sum_{n \in \mathcal{N}} a_{u,m_l} r_{u,m_l}(n) \geq r_{\text{th}}, \quad \forall u \in \mathcal{U}, \forall m_l \in \mathcal{M}_l, \quad (39)$$

where r_{th} is the minimum data rate requirement of each LUE. The downlink transmit power of each ABSs u for associated LUEs should be remain within the power budget limits:

$$0 \leq a_{u,m_l} p_{u,m_l}(n) \leq p_{\max}, \quad \forall u \in \mathcal{U}, m_l \in \mathcal{M}_l, n \in \mathcal{N}, \quad (40)$$

To ensure a safe distance between the U ABS, we define a secure distance that can avoid an overlap in their coverage region. This threshold distance can be defined for all ABSs $\forall i, j \in \mathcal{U}$:

$$\|\mathbf{d}_i(n) - \mathbf{d}_j(n)\|^2 \geq d_{\text{th}}, \quad \forall i, j \in \mathcal{U}, i \neq j. \quad (41)$$

Each ABS u can assign each resource block k at each time slot n to a maximum of one LUE that can be given as:

$$\sum_{u=1}^U \sum_{k=1}^K \sum_{m_l=1}^{M_l} a_{u,k,m_l}(n) \leq 1, \quad \forall n \in \mathcal{N}, \quad (42)$$

$$a_{u,k,m_l}(n) \in \{0, 1\}, \quad \forall u \in \mathcal{U}, \forall k \in \mathcal{K}, \forall m_l \in \mathcal{M}_l.$$

In addition, each ABS u can be associated with atmost one backhaul service node, depending on its position in the sea, which can be defined as:

$$\sum_{u=1}^U a_{s,u}(n) \leq 1, \quad a_{s,u}(n) \in \{0, 1\}, \quad \forall n \in \mathcal{N}, \quad (43)$$

$$\sum_{c=1}^C \sum_{u=1}^U a_{c,u}(n) \leq 1, \quad a_{c,u}(n) \in \{0, 1\}, \quad \forall n \in \mathcal{N},$$

The satellite s can assign each resource block z at each time slot n to a maximum of one HUE or ABS for backhaul that can be given as respectively:

$$\sum_{z=1}^Z \sum_{m_h=1}^{M_h} a_{s,z,m_h}(n) \leq 1, \quad \forall n \in \mathcal{N}, \quad (44)$$

$$a_{s,z,m_h}(n) \in \{0, 1\}, \quad \forall k \in \mathcal{K}, \forall m_h \in \mathcal{M}_h,$$

$$\sum_{z=1}^Z \sum_{u=1}^U a_{s,z,u}(n) \leq 1, \quad \forall n \in \mathcal{N}, \quad (45)$$

$$a_{s,z,u}(n) \in \{0, 1\}, \quad \forall k \in \mathcal{K}, \forall u \in \mathcal{U}.$$

Similarly, each CBS c can assign each resource block y at each time slot n to a maximum of one HUE or ABS for backhaul that can be given as respectively:

$$\sum_{c=1}^C \sum_{y=1}^Y \sum_{m_h=1}^{M_h} a_{c,y,m_h}(n) \leq 1, \quad \forall n \in \mathcal{N}, \quad (46)$$

$$a_{c,y,m_h}(n) \in \{0, 1\}, \quad \forall c \in \mathcal{C}, y \in \mathcal{Y}, \forall m_h \in \mathcal{M}_h,$$

$$\sum_{c=1}^C \sum_{y=1}^Y \sum_{u=1}^U a_{c,y,u}(n) \leq 1, \quad \forall n \in \mathcal{N}, \quad (47)$$

$$a_{c,y,u}(n) \in \{0, 1\}, \quad \forall c \in \mathcal{C}, \forall y \in \mathcal{Y}, \forall u \in \mathcal{U}.$$

The large transmission distances between the satellite and ABSs are assumed to be constant at each time slot n due to the short interval. The satellite and CBSs must meet the downlink demand of associated HUEs i.e.:

$$\sum_{n \in \mathcal{N}} a_{s,m_h} r_{s,m_h}(n) \geq r_{th}, \quad \forall m_h \in \mathcal{M}_h, \quad (48)$$

$$\sum_{n \in \mathcal{N}} a_{c,m_h} r_{c,m_h}(n) \geq r_{th}, \quad \forall c \in \mathcal{C}, \forall m_h \in \mathcal{M}_h, \quad (49)$$

where r_{th} is each HUE datarate requirement threshold, respectively. Similarly, the downlink transmit power of satellite s for associated devices in each z RB should remain within the power budget limits:

$$0 \leq a_{s,u} p_{s,u}(n) \leq p_{max}, \quad \forall n \in \mathcal{N}, \forall u \in \mathcal{U}, \quad (50)$$

$$0 \leq a_{s,m_h} p_{s,m_h}(n) \leq p_{max}, \quad \forall m_h \in \mathcal{M}_h, \forall n \in \mathcal{N}. \quad (51)$$

The downlink transmit power of each CBS c for associated devices in each y RB should remain within the power budget limits:

$$0 \leq a_{c,u} p_{c,u}(n) \leq p_{max}, \quad \forall c \in \mathcal{C}, \forall u \in \mathcal{U}, \forall n \in \mathcal{N}, \quad (52)$$

$$0 \leq a_{c,m_h} p_{c,m_h}(n) \leq p_{max}, \quad \forall c \in \mathcal{C}, \forall m_h \in \mathcal{M}_h, \forall n \in \mathcal{N}. \quad (53)$$

A. Problem Formulation

Given the network specifics described above, our objective is to establish an efficient allocation of resources and a maritime UE association scheme that will maximize the EE of the network while meeting the request for user data services within a limited period. We can define the total network EE (Bit/Joule) as follows:

$$\eta_{EE}(n) = \frac{R_t(n)}{P_t^+(n)}, \quad (54)$$

where R_t indicates the total data rate and P_t^+ indicates the non-negative power needed to transmit this data and operate the network nodes at time slot n . For the sake of understanding, we can define a separate EE for each network node. The EE of U ABSs at time slot n can be defined as follows:

$$\eta_u(n) = \frac{R_u(n)}{P_u^+(n)} = \sum_{\mathcal{U}} \sum_{\mathcal{M}_l} \left(\frac{r_{u,m_l}(n)}{p_{u,m_l}(n) + p^{\text{flight}}} \right), \quad \forall n \in \mathcal{N}. \quad (55)$$

The EE of satellite s at time slot n can be defined as:

$$\eta_s(n) = \frac{R_s(n)}{P_s^+(n)} = \sum_{\mathcal{U}} \sum_{\mathcal{M}_h} \left(\frac{r_{s,u}(n) + r_{s,m_h}(n)}{p_{s,u}(n) + p_{s,m_h}(n) + p_s^{\text{circuit}}} \right) \quad \forall n \in \mathcal{N}. \quad (56)$$

Similarly, the EE of C CBS at time slot n can be stated as follows:

$$\eta_c(n) = \frac{R_c(n)}{P_c^+(n)} = \sum_{\mathcal{C}} \sum_{\mathcal{U}} \sum_{\mathcal{C}} \left(\frac{r_{c,u}(n) + r_{c,m_h}(n)}{p_{c,u}(n) + p_{c,m_h}(n) + p_c^{\text{circuit}}} \right), \quad \forall n \in \mathcal{N}. \quad (57)$$

Thus, the total network EE can now be define as:

$$\eta_{EE}(n) = \eta_u(n) + \eta_s(n) + \eta_c(n), \quad \forall n \in \mathcal{N}. \quad (58)$$

According to the above analysis, the optimization problem of both HUEs and LUEs association, resource allocation, and ABSs deployment for maximizing the SAS network EE can be formulated as follows:

$$\begin{aligned} \max_{\mathbf{a}, \mathbf{p}, \mathbf{d}_u} \quad & \eta_{EE}, \\ \text{s.t.} \quad & (31) - (53), \end{aligned} \quad (59)$$

where η_{EE} is given in (54). The objective function in (59) is a function of users' association \mathbf{a} , transmission power \mathbf{p} , and the ABS 3D deployment \mathbf{d}_n . In the given problem, the UEs association constraints in (42), (44), and (46) are integer (binary) constraints. Similarly, the ABS selection constraints in (43), (45), and (47), are also integer constraints, and the objective function in (59) is in fractional form, which makes this problem a mixed integer non-convex fractional optimization problem. Moreover, the problem is combinatorial due to the association (binary) constraints in (42), (44), and (46). In fact, this problem is a non-deterministic polynomial-time hard (NP-hard) problem.

V. PROPOSED SOLUTION

In this section, we will present our proposed algorithm based on the BD, DA, ADMM, and Gurobi optimizer [63]. We developed our algorithm architecture based on the BD structure. Then we solve the master problem by using the Gurobi optimization solver. In the sub-problem, the DA is used to handle fractional programming. We use ADMM to provide a distributed solution in the inner loop of the DA. Details are given in the following subsections.

The main challenge of solving the problem (59) is the non-concavity caused by the fractional form of the objective function and non-convexity due to maritime UEs association (binary) variables constraints given in (42), (44), and (46), and ABSs backhaul selection variable given in (43), (45), and (47). In order to obtain the solution to this problem, we first decompose (59) into three subproblems by taking advantage of

its block separability. Thus, the first subproblem is established for the ABS EE at each time slot n , as follows:

$$\begin{aligned} \max_{\mathbf{a}_u, \mathbf{p}_u, \mathbf{d}_u} \quad & \eta_u(n), \\ \text{s.t.} \quad & (31) - (43), \end{aligned} \quad (60)$$

The second subproblem is established for the satellite EE at each time slot n , as follows:

$$\begin{aligned} \max_{\mathbf{a}_s, \mathbf{p}_s} \quad & \eta_s(n), \\ \text{s.t.} \quad & (44), (45), (48), (50), (51). \end{aligned} \quad (61)$$

The third subproblem is established for the CBSs EE at each time slot n , as follows:

$$\begin{aligned} \max_{\mathbf{a}_c, \mathbf{p}_c} \quad & \eta_c(n), \\ \text{s.t.} \quad & (46), (47), (49), (52), (53). \end{aligned} \quad (62)$$

We next tackle each problem individually.

A. Aerial Base Stations Energy Efficiency (ABSs-EE)

This part introduces an optimization scheme of LUEs' association, transmit power control, and ABSs' deployment for (60). This optimization algorithm describes maximizing the ABSs' energy efficiency in the SAS-NTN networks based on BD, DA, ADMM, and optimization solver.

1) *Bender Decomposition for ABS EE*: The BD algorithm is a solution approach for tackling constraints in optimization problems based on the idea of partition and delayed constraint generation [64]. Firstly, a mathematical problem formulation is proposed [64] as MINLP, then decompose the problem in two parts:

- A master problem, which deals with binary constraints by branch and bound (B&B) technique, finds values for a subset of the original variables and associated constraints.
- One or more subproblems are used to find the solution for the remaining original variables by any linear programming (LP) method while keeping the master problem variables constant.

Both problems are solved iteratively until convergence. In the master problem, there are some added constraints called the Benders Cut to cut the solution region. When the upper and lower bounds meet or the difference between them is lower than a certain threshold, the optimal solution will be given.

Initialization: We first assume that the master problem has a trivial solution and can be solved by generating the initialization in the given problem. Then, we need to assign the loop counter, i.e., $i_u = 1$. In our problem, we have an association variable a_u in binary form, and, thus, the upper and lower bounds will be $a_{UB} = 1$ and $a_{LB} = 0$ respectively. Moreover, we implement a function χ_u as an auxiliary variable, representing the objective function of the subproblems within the objective function of the master problem. We can set the initial value for a function χ_u^ψ as χ_u^{down} , to avoid an unbounded solution in the first iteration when there is no cut in the master problem. It can be initiated with a negative value, i.e., -10^6 .

Subproblems: The idea behind the construction of subproblems is to fix the value of association variables \mathbf{a}_u to avoid them. Therefore, we can express the subproblem as given in (63). We can represent the dual variable for the fronthaul constraints in each ABS u that fixed association variables values, i.e., $\kappa_{u,m_l}^{i_u}$ from ABS u to LUE m_l and backhaul constraints $\kappa_{s,u}^{i_u}$ and $\kappa_{c,u}^{i_u}$ form the satellite s and CBS c to ABS u respectively. Hence, the subproblem can be obtained with only transmit power and ABSs' deployment continuous variables, and it can be represented as:

$$\max_{\mathbf{p}_u, \mathbf{d}_u} \quad \tilde{\eta}_u, \quad (63a)$$

$$\text{s.t.} \quad \tilde{\eta}_u = \frac{R_u(\tilde{\mathbf{a}}_u, \mathbf{p}_u, \mathbf{d}_u)}{P_u^+}, \quad (63b)$$

$$\mathbf{a}_{u,m_l} = \mathbf{a}_{u,m_l}^{i_u} : \kappa_{u,m_l}^{i_u}, \quad u \in \mathcal{U}, \forall m_l \in \mathcal{M}_l, \quad (63c)$$

$$\mathbf{a}_{s,u} = \mathbf{a}_{s,u}^{i_u} : \kappa_{s,u}^{i_u}, \quad \forall u \in \mathcal{U}, \quad (63d)$$

$$\mathbf{a}_{c,u} = \mathbf{a}_{c,u}^{i_u} : \kappa_{c,u}^{i_u}, \quad c \in \mathcal{C}, \forall u \in \mathcal{U}, \quad (63e)$$

$$(31) - (41), \quad (63f)$$

where $\tilde{\mathbf{a}}_u$ the fixed value of each association vector from the initial master problem solution, and this fixing value constraint is stated in (63c), (63d), and (63e). After solving this subproblem, we will get the sub-optimal transmit power \mathbf{p}_u^* and the deployment vector \mathbf{d}_u^{*4} for each ABS u . This obtained subproblem will be solved by utilizing DA in Section V-A2.

Convergence Analysis and Bounds: This process is used to derive upper and lower bounds that are used as the stopping criterion for the algorithm and as a condition for the convergence. In this step, we obtain the upper and lower bound difference. The objective function at iteration i_u provides the upper bound, which is stated as:

$$\eta_{UB}^{i_u} = \frac{\tilde{R}_u(\mathbf{a}_u^{i_u}, \mathbf{p}_u^{i_u}, \mathbf{d}_u^{i_u})}{\tilde{P}_u(\mathbf{a}_u^{i_u}, \mathbf{p}_u^{i_u}, \mathbf{d}_u^{i_u})^+}, \quad (64)$$

where \tilde{R}_u and \tilde{P}_u are intermediate values of both parameters at iteration i_u which depend on the sum rate from all associated LUEs and transmit power consumption respectively. The lower bound can be given as:

$$\eta_{LB}^{i_u} = \chi_u^{i_u}. \quad (65)$$

Therefore, the stopping criterion can be stated as:

$$\begin{cases} \eta_{UB}^{i_u} - \eta_{LB}^{i_u} \leq \epsilon, & \text{stop,} \\ \text{otherwise,} & \text{continue,} \end{cases} \quad (66)$$

where ϵ is a pre-defined tolerance parameter. Thus, after convergence the sub-optimal values of \mathbf{a}_u^* , \mathbf{p}_u^* and \mathbf{d}_u^* can be obtained.

Master Problem: This problem deals only with association variables while all other variables remain fixed. The loop

⁴Hereinafter, the ABSs' deployment vector can be alternatively used with these notations, i.e., $\mathbf{d}_u = \{x_u, y_u\}$.

counter can be update as $i_u = i_u + 1$, and after that the solvable problem become as follows:

$$\max_{\mathbf{a}_u, \chi_u} \chi_u, \quad (67a)$$

$$\text{s.t.} \quad (42), (43) \quad (67b)$$

$$(69), \quad (67c)$$

$$\chi_u \geq \chi^{\text{down}}, \quad (67d)$$

where inequality constraint in (67c) represents the Bender cut in the master problem. At every iteration, the new Benders cut will generate and append to the master problem. Additionally, the previous iteration's Bender cuts remain the same in the master problem. The master problem becomes the mixed integer programming problem which only decides the associations and this can be solved with an optimization solver to reduce the complexity. At each iteration, we obtain the optimal values of association \mathbf{a}_u^* and auxiliary variable χ_u .

After each iteration of the master problem, we solve the subproblem again using the obtained local optimal values. Therefore, when the optimal criterion of upper and lower is met, the iteration process will stop. These details of the Benders technique are presented in Algorithm 1. After getting the optimal user association \mathbf{a}_u^* , the subproblem is still non-convex due to its objective function. Note that the objective function is non-convex in (63b). Therefore, we apply the Taylor approximation to the numerator term in (63b) to linearize the objective function as given in equation (68).

Lemma 1. Since the first-order Taylor approximation is the global lowest bound of a convex function and the global upper bound of a concave function [65].

Proof: See Appendix A.

2) *Dinkelbach Algorithm for ABS EE:* We use the DA to address the fractional nature of the objective function. Fortunately, this method will always converge to local optima [66]. The DA is widely adopted in solving the fractional programming [67]. It can be observed from (63) that it has a fractional objective function. Therefore, we can employ nonlinear fractional programming to transform the original problem in fractional from into an equivalent subtractive form. Without loss of generality, the system maximum average EE can be given as:

$$\tilde{\eta}_u^* = \frac{R_{u,m_l}^{lb}(\tilde{\mathbf{a}}_u^*, \mathbf{p}_u^*, \mathbf{d}_u^*)}{P_u^+} = \arg \max_{\mathbf{p}_u, \mathbf{d}_u} \frac{R_{u,m_l}^{lb}(\tilde{\mathbf{a}}_u^*, \mathbf{p}_u, \mathbf{d}_u)}{P_u^+}, \quad (71)$$

Algorithm 1 Outer Loop Bender Decomposition

- 1: **Input:** Initialize variables $\tilde{\mathbf{a}}$, loop counter i_u , $\chi_u^\psi = \chi^{\text{down}}$
 - 2: **Output:** optimal solution \mathbf{a}_u^* , \mathbf{p}_u^* , and \mathbf{d}_u^*
 - 3: **while** $\eta_{\text{UB}}^{i_u} - \eta_{\text{LB}}^{i_u} \geq \epsilon$ **do**
 - 4: **Subproblem**
 - 5: obtain \mathbf{p}_u^* and \mathbf{d}_u^* using Dinkelbach algorithm
 - 6: **Bounds calculation**
 - 7: calculate upper and lower bounds $\eta_{\text{UB}}^{i_u}$ and $\eta_{\text{LB}}^{i_u}$ by (64) and (65)
 - 8: **Master Problem**
 - 9: step 1: Increment in loop counter $i_u = i_u + 1$
 - 10: step 2: Add the new Bender cut in (67)
 - 11: step 3: Solve the updated master problem in (67)
 - 12: step 4: Acquire the optimal value \mathbf{a}_u^* and χ_u
 - 13: **end while**
-

then, we introduce a Remark 1 to solve the optimization problem in (63).

Remark 1. When $R_{u,m_l}^{lb}(\tilde{\mathbf{a}}_u, \mathbf{p}_u, \mathbf{d}_u) \geq 0$ and $P_u^+ > 0$ is fulfilled, the objective function in (63) can be rewritten to a parametric subtractive form equivalently if and only if the following condition is satisfied:

$$\begin{aligned} \max_{\mathbf{p}_u, \mathbf{d}_u} R_{u,m_l}^{lb}(\tilde{\mathbf{a}}_u^*, \mathbf{p}_u, \mathbf{d}_u) - \eta_u^* P_u^+ \\ = R_{u,m_l}^{lb}(\tilde{\mathbf{a}}_u^*, \mathbf{p}_u^*, \mathbf{d}_u^*) - \eta_u^* P_u^+. \end{aligned} \quad (72)$$

This Remark 1 illustrates that there exists an equivalent transformed problem with an objective function in subtractive form, which leads to the same maximum η_u^* obtained by directly solving (63). Our objective function is a strictly monotonic increasing function of η_u which can be stated as:

$$F(\mathbf{a}_u, \mathbf{p}_u, \mathbf{d}_u; \eta_u) = R_{u,m_l}^{lb}(\tilde{\mathbf{a}}_u, \mathbf{p}_u, \mathbf{d}_u) - \eta_u P_u^+. \quad (73)$$

Thus, the equivalent optimization problem in subtractive form is reformulated as:

$$\begin{aligned} \max_{\mathbf{p}_u, \mathbf{d}_u} F(\tilde{\mathbf{a}}_u, \mathbf{p}_u, \mathbf{d}_u; \eta_u), \\ \text{s.t.} \quad (63b) - (63f). \end{aligned} \quad (74)$$

The nonlinear fractional objective function is transformed into a subtractive objective function, which is a multi-objective convex optimization problem whereby the variable η_u (non-negative) can be regarded as a negative weight of \mathbf{p}_u . At last, parameter η_u updates itself after each iteration and finally obtains the sub-optimality condition, which can be defined as

$$R_{u,m_l}^{lb} = \sum_{u=1}^U \sum_{m_l=1}^{M_l} \tilde{\mathbf{a}}_{u,m_l} B_{u,m_l} \left[\log_2 \left\{ 1 + \frac{p_{u,m_l} g_0}{(\Omega_{u,m_l} + \sigma^2) (\|\mathbf{d}_{u,\text{local}}(n) - \mathbf{d}_{m_l}(n)\|^2)} \right\} - \frac{p_{u,m_l} g_0 \{ \|\mathbf{d}_u(n) - \mathbf{d}_{m_l}(n)\|^2 - \|\mathbf{d}_{u,\text{local}}(n) - \mathbf{d}_{m_l}(n)\|^2 \} \log_2 e}{\{ \|\mathbf{d}_{u,\text{local}}(n) - \mathbf{d}_{m_l}(n)\|^2 \} \{ p_{u,m_l} g_0 + (\Omega_{u,m_l} + \sigma^2) (\|\mathbf{d}_{u,\text{local}}(n) - \mathbf{d}_{m_l}(n)\|^2) \}} \right] \quad (68)$$

$$\chi_u \leq \eta_{\text{UB}}^{i_u} + \sum_{u=1}^U \sum_{m_l=1}^{M_l} \kappa_{u,m_l}^{i_u} (\mathbf{a}_{u,m_l} - \mathbf{a}_{u,m_l}^{i_u}) + \sum_{u=1}^U \kappa_{s,u}^{i_u} (\mathbf{a}_{s,u} - \mathbf{a}_{s,u}^{i_u}) + \sum_{c=1}^C \sum_{u=1}^U \kappa_{c,u}^{i_u} (\mathbf{a}_{c,u} - \mathbf{a}_{c,u}^{i_u}), \quad (69)$$

$$f(\mathbf{d}_u)^{lb} = \|\mathbf{d}_{u1,\text{local}} - \mathbf{d}_{u2,\text{local}}\|^2 + 2(\mathbf{d}_{u1,\text{local}} - \mathbf{d}_{u2,\text{local}})(\mathbf{d}_{u1} - \mathbf{d}_{u2})^T. \quad (70)$$

Algorithm 2 Inner Loop Dinkelbach Algorithm

```

1: Input: loop counter  $j = 0$ , energy efficiency  $\eta_u = 0$ ,
   maximum tolerance  $\Upsilon$ 
2: Output: optimal power  $\mathbf{p}_u^*$ , and UAVs deployment  $\mathbf{d}_u^*$ 
3: Maximum energy efficiency  $= \eta_u^*$ 
4: while  $\|F(\mathbf{a}_u, \mathbf{p}_u, \mathbf{d}_u; \eta_u) \geq \Upsilon\|$  do
5:   Solve the subproblem (74) by ADMM to find the
   optimal solution  $\mathbf{p}_u^*$  and  $\mathbf{d}_u^*$  with  $\eta_u$ 
6:   Calculate  $\eta_u = \frac{R_u}{P_u}$  with obtained  $\mathbf{p}_u^*$  and  $\mathbf{d}_u^*$ 
7:   Calculate new  $F(\mathbf{a}_u, \mathbf{p}_u, \mathbf{d}_u; \eta_u)$  with updated  $\eta_u$ ,  $\mathbf{p}_u^*$ 
   and  $\mathbf{d}_u^*$ 
8:   Update loop counter  $j = j + 1$ 
9: end while

```

η_u^* . The details of DA are provided in Algorithm 2. The safe distance constraint is given in (41) between ABSs is of the quadratic type. Therefore, we provide the following lemma 2 to linearize it.

Lemma 2. We can linearize this constraint by approximating it with first-order Taylor expansion, which can also be the lower bound for the distance threshold as given in (70).

Proof: See Appendix B.

3) *ADMM for ABS EE:* For the subproblem, we use ADMM to solve it in a distributed way. An ADMM is commonly used to decouple the constraint linked with all ABSs. The original problem also costs a great deal of time and resources. By splitting the problem into small problems, time and money can be saved in green communication.

Firstly, we need to turn (74) into a solvable problem. In this subproblem, we introduce three auxiliary variables ω_u , ν_u and o_u as global copies, which implies that three new equality constraints are applied to the subproblem (74), which can be given as:

$$\mathbf{p}_u = \omega_u, \quad \forall u \in \mathcal{U}, \quad (75a)$$

$$x_u = \nu_u, \quad \forall u \in \mathcal{U}, \quad (75b)$$

$$y_u = o_u, \quad \forall u \in \mathcal{U}, \quad (75c)$$

where ω_u is the global copy of transmit power variables. Similarly, ν_u and o_u are the global copies of x and y coordinates' decision variables for each ABS deployment, respectively. Therefore, the ABS's deployment vector \mathbf{d}_u in a global problem can be represented by Θ_u . Thus, we can find that constraints (40) and (41) are involved in all the ABSs. The corresponding subproblem (74) is then reformulated as:

$$\max_{\mathbf{p}_u, \omega_u, \mathbf{d}_u, o_u} F(\tilde{\mathbf{a}}_u, \mathbf{p}_u, \mathbf{d}_u; \eta_u), \quad (76a)$$

$$\text{s.t. } 0 \leq a_{u, m_l} \omega_{u, m_l}(n) \leq p_{\max}, \quad \forall u, m_l, \quad (76b)$$

$$\sum_{i, j \in \mathcal{U}, i \neq j} f(\Theta_u)^{lb} \geq d_{\text{th}}, \quad (76c)$$

$$(31) - (39), \quad (76d)$$

$$(63b) - (63f), \quad (76e)$$

$$(75a) - (75c). \quad (76f)$$

The problem's augmented Lagrangian function is given by

Algorithm 3 ADMM Distributed Algorithm for Subproblem

```

1: Input: Initialize variables  $t, \phi, \mathbf{\Pi}, \rho$ ,
2: while the criterion to stop is not met do
3:   Central Controller Update
4:   continue
5:   wait
6:   until obtained updated  $\phi_u, \mathbf{\Pi}_u, \Xi_u, \mathbf{p}_u, \mathbf{d}_u$  from all
   ABSs
7:   step 1: Solve problem (80) and find the optimal
    $\tilde{\omega}_u$  and  $\tilde{\Theta}_u$ 
8:   step 2: Send these  $\tilde{\omega}_u$  and  $\tilde{\Theta}_u$  to all ABSs
9:   step 3: Update the variable  $t = t+1$ 
10:
11: ABSs Updates
12: continue
13: wait
14: until from the central controller, obtained updated  $\tilde{\omega}_u$ 
and  $\tilde{\Theta}_u$ 
15: step 1: Solve (81), and find the optimal solution
 $\tilde{\mathbf{p}}$  and  $\tilde{\mathbf{d}}$ 
16: step 2: All fix valued constraints on dual variables
update:

$$\phi_u[t+1] = \phi_u[t] + \rho(\tilde{\omega}_u - \tilde{p}_u)$$


$$\mathbf{\Pi}_u[t+1] = \mathbf{\Pi}_u[t] + \rho(\tilde{\nu}_u - \tilde{x}_u)$$


$$\Xi_u[t+1] = \Xi_u[t] + \rho(\tilde{o}_u - \tilde{y}_u)$$

17: step 3: Send updated  $\tilde{\mathbf{p}}, \tilde{\mathbf{d}}, \phi_u[t+1], \mathbf{\Pi}_u[t+1]$  and
 $\Xi_u[t+1]$  to the central controller for upcoming
iteration
18: end while

```

(77). We consider that the global copy variables ω_u and Θ_u are managed by the central controller, and the variables \mathbf{p}_u and \mathbf{d}_u are processed locally by the ABSs. Based on the above analysis, the global consensus problem for finding global variables ω_u and Θ_u is formulated as follows:

$$\min_{\omega_u, \Theta_u} (78), \quad (80a)$$

$$\text{s.t. } 0 \leq a_{u, m_l} \omega_{u, m_l}(n) \leq p_{\max}, \quad \forall u, m_l, \quad (80b)$$

$$\sum_{i, j \in \mathcal{U}, i \neq j} f(\Theta_u)^{lb} \geq d_{\text{th}}, \quad (80c)$$

where $\tilde{\mathbf{p}}_u$, $\tilde{\mathbf{x}}_u$ and $\tilde{\mathbf{y}}_u$ indicate the constant values which can be obtained by ABSs' update. Therefore, to update \mathbf{p}_u , \mathbf{x}_u and \mathbf{y}_u , we need to solve the following problem at each ABS u :

$$\min_{\mathbf{p}_u, \mathbf{d}_u} (79), \quad (81a)$$

$$\text{s.t. } (31) - (39), \quad (81b)$$

$$(63b) - (63e). \quad (81c)$$

where $\tilde{\omega}_u$, $\tilde{\nu}_u$ and \tilde{o}_u indicate the fixed values which can be obtained by the central controller's update. Therefore, the dual

variables ϕ_u , Π_u , and Ξ_u can be updated at each ABS u by the following equation:

$$\phi_u[t+1] = \phi_u[t] + \rho(\tilde{\omega}_u - \tilde{p}_u), \quad (82a)$$

$$\Pi_u[t+1] = \Pi_u[t] + \rho(\tilde{\nu}_u - \tilde{x}_u), \quad (82b)$$

$$\Xi_u[t+1] = \Xi_u[t] + \rho(\tilde{o}_u - \tilde{y}_u). \quad (82c)$$

The summary of this ADMM is depicted in Algorithm 3 and the solution process is shown in Fig. 2. We have decomposed and provided iterative algorithms for ABS EE (60). As we discussed the solution algorithm in detail in earlier sections, in the upcoming problems, these same algorithms will be applied directly to the respective problems without any explanation.

B. Satellite Energy Efficiency (Sat-EE)

This section deals with the satellite EE maximization problem (61) by utilizing the same previous algorithms. Firstly, BD will apply to decompose, and then DA will transform the subproblem objective into a subtractive form. After that, ADMM will solve the subproblem, which is given as follows:

1) *Bender Decomposition for Sat-EE*: First, the loop counter, i.e., $i_s = 1$ is initialize. Then the variables \mathbf{a}_s for U ABSs, and M_h HUEs association is initialized with the upper bound $a_{\text{UB}} = 1$ lower bound $a_{\text{LB}} = 0$. Moreover, the function χ_s as an auxiliary variable, representing the objective function of a subproblem within the master problem's objective function, whose unitize value can be set as $\chi_s = 10^{-6}$ to avoid an unbounded solution.

Subproblem: We can express the dual variable for the ABSs and HUEs association, i.e., $\kappa_{s,u}$ and κ_{s,m_h} , respectively. Thus, the subproblem can be define as:

$$\max_{\mathbf{p}_s} \tilde{\eta}_s, \quad (83a)$$

$$\text{s.t. } \tilde{\eta}_s = \frac{R_s(\tilde{\mathbf{a}}_s, \mathbf{p}_s)}{P_s^+}, \quad (83b)$$

$$\mathbf{a}_{s,u} = \mathbf{a}_{s,u}^{i_s} : \kappa_{s,u}^{i_s}, \quad u \in \mathcal{U}, \quad (83c)$$

$$\mathbf{a}_{s,m_h} = \mathbf{a}_{s,m_h}^{i_s} : \kappa_{s,m_h}^{i_s}, \quad \forall m_h \in \mathcal{M}_h, \quad (83d)$$

$$(48), (50), (51). \quad (83e)$$

Convergence Analysis and Bounds: The objective function at iteration ψ provides the upper bound, which is stated as:

$$\eta_{\text{UB}}^{i_s} = \frac{\tilde{R}_s(\mathbf{a}_s^{i_s}, \mathbf{p}_s^{i_s})}{\tilde{P}_s(\mathbf{a}_s^{i_s}, \mathbf{p}_s^{i_s})^+}. \quad (84)$$

The lower bound can be define as follows:

$$\eta_{\text{LB}}^{i_s} = \chi_s^{i_s}. \quad (85)$$

Thus, the stopping criterion can be stated as:

$$\begin{cases} \eta_{\text{UB}}^{i_s} - \eta_{\text{LB}}^{i_s} \leq \epsilon, & \mathbf{stop}, \\ \text{otherwise,} & \mathbf{continue}, \end{cases} \quad (86)$$

Master Problem: The loop counter updates as $i_s = i_s + 1$, and after that, the solvable problem becomes as follows:

$$\max_{\mathbf{a}_s, \chi_s} \chi_s, \quad (87a)$$

$$\text{s.t. } (44), (45), \quad (87b)$$

$$\begin{aligned} \chi_s &\leq \eta_{\text{UB}}^{i_s} + \sum_{u=1}^U \kappa_{s,u}^{i_s} (\mathbf{a}_{s,u} - \mathbf{a}_{s,u}^{i_s}) \\ &+ \sum_{m_h=1}^{M_h} \kappa_{s,m_h}^{i_s} (\mathbf{a}_{s,m_h} - \mathbf{a}_{s,m_h}^{i_s}), \end{aligned} \quad (87c)$$

$$\chi_s \geq \chi^{\text{down}}, \quad (87d)$$

2) *Dinkelbach Algorithm for Sat-EE*: The objective function in the satellite subproblem can be transformed as follows:

$$F(\mathbf{a}_s, \mathbf{p}_s; \eta_s) = R_s(\tilde{\mathbf{a}}_s, \mathbf{p}_s) - \eta_s P_s^+. \quad (88)$$

Thus, the equivalent optimization problem in subtractive form is reformulated as:

$$\begin{aligned} \max_{\mathbf{p}_s} F(\tilde{\mathbf{a}}_s, \mathbf{p}_s; \eta_s), \\ \text{s.t. } (48), (50), (51). \end{aligned} \quad (89)$$

3) *ADMM for Sat-EE*: In this subproblem problem, we introduce an auxiliary variable ω_s as a global copy, which implies that a new equality constraint is applied to the subproblem (89), which can be given as:

$$\mathbf{p}_s = \omega_s. \quad (90)$$

We can find that constraints (50) and (51) are involved in all the satellite's associated nodes. The corresponding subproblem (74) is then reformulated as:

$$\max_{\mathbf{p}_s, \omega_s} F(\tilde{\mathbf{a}}_s, \mathbf{p}_s; \eta_s), \quad (91a)$$

$$\text{s.t. } 0 \leq a_{s,u} \omega_{s,u}(n) \leq p_{\text{max}}, \quad \forall u, \quad (91b)$$

$$0 \leq a_{s,m_h} \omega_{s,m_h}(n) \leq p_{\text{max}}, \quad \forall m_h, \quad (91c)$$

$$(48). \quad (91d)$$

$$\mathcal{L} = F(\tilde{\mathbf{a}}_u, \mathbf{p}_u, \mathbf{d}_u; \eta_u) + \sum_{u=1}^U (\phi_u(\mathbf{p}_u - \omega_u) + \Pi_u(x_u - \nu_u) + \Xi_u(y_u - o_u)) + \frac{\rho}{2} \sum_{u=1}^U (\|\mathbf{p}_u - \omega_u\|_2^2 + \|x_u - \nu_u\|_2^2 + \|y_u - o_u\|_2^2), \quad (77)$$

$$F(\tilde{\mathbf{a}}_u, \mathbf{p}_u, \mathbf{x}_u, \mathbf{y}_u; \eta_u) + \sum_{u=1}^U (\phi_u(\tilde{\mathbf{p}}_u - \omega_u) + \Pi_u(\tilde{x}_u - \nu_u) + \Xi_u(\tilde{y}_u - o_u)) + \frac{\rho}{2} \sum_{u=1}^U (\|\tilde{\mathbf{p}}_u - \omega_u\|_2^2 + \|\tilde{x}_u - \nu_u\|_2^2 + \|\tilde{y}_u - o_u\|_2^2), \quad (78)$$

$$F(\tilde{\mathbf{a}}_u, \mathbf{p}_u, x_u, y_u; \eta_u) + \phi_u(\mathbf{p}_u - \tilde{\omega}_u) + \Pi_u(x_u - \tilde{\nu}_u) + \Xi_u(y_u - \tilde{o}_u) + \frac{\rho}{2} (\|\mathbf{p}_u - \tilde{\omega}_u\|_2^2 + \|x_u - \tilde{\nu}_u\|_2^2 + \|y_u - \tilde{o}_u\|_2^2), \quad (79)$$

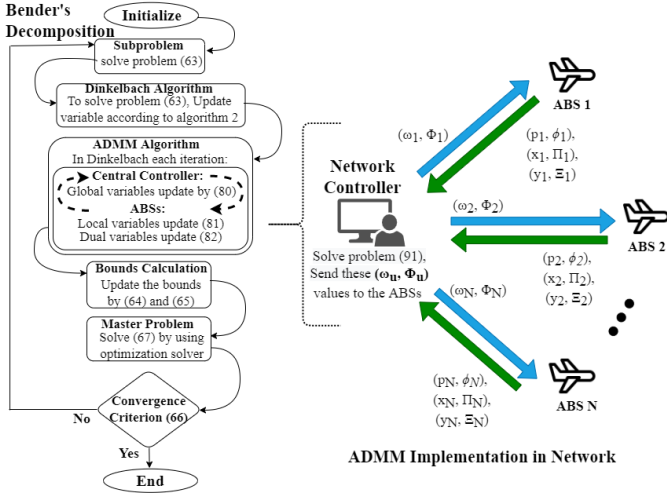


Figure 2: Illustration of Bender decomposition, Dinkelbach algorithm, and ADMM working procedure for ABSs.

The problem's augmented Lagrangian function can be define as follows:

$$\mathcal{L} = F(\tilde{\mathbf{a}}_s, \mathbf{p}_s; \eta_s) + (\phi_s(\mathbf{p}_s - \boldsymbol{\omega}_s)) + \frac{\rho}{2} (\|\mathbf{p}_s - \boldsymbol{\omega}_s\|_2^2) \quad (92)$$

We consider that the global copy variables $\boldsymbol{\omega}_s$ are managed by the central controller, and the variables \mathbf{p}_s are processed locally by the satellite. Based on the above analysis, the global consensus problem for finding global variables $\boldsymbol{\omega}_s$ is formulated as follows:

$$\min_{\boldsymbol{\omega}_s} F(\tilde{\mathbf{a}}_s, \mathbf{p}_s; \eta_s) + (\phi_s(\tilde{\mathbf{p}}_s - \boldsymbol{\omega}_s)) + \frac{\rho}{2} (\|\tilde{\mathbf{p}}_s - \boldsymbol{\omega}_s\|_2^2), \quad (93a)$$

$$\text{s.t. } 0 \leq a_{s,u} \omega_{s,u}(n) \leq p_{\max}, \quad \forall u, \quad (93b)$$

$$0 \leq a_{s,m_h} \omega_{s,m_h}(n) \leq p_{\max}, \quad \forall m_h, \quad (93c)$$

where $\tilde{\mathbf{p}}_s$ indicates the constant values which can be obtained by the satellite's update. Therefore, to update \mathbf{p}_s , we need to solve the following problem at satellite:

$$\min_{\mathbf{p}_s} F(\tilde{\mathbf{a}}_s, \mathbf{p}_s; \eta_s) + (\phi_s(\mathbf{p}_s - \tilde{\boldsymbol{\omega}}_s)) + \frac{\rho}{2} (\|\mathbf{p}_s - \tilde{\boldsymbol{\omega}}_s\|_2^2), \quad (94a)$$

$$\text{s.t. } (48). \quad (94b)$$

where $\tilde{\boldsymbol{\omega}}_s$ indicates the fixed value which can be obtained by the central controller's update. Therefore, the dual variable ϕ_u can be updated at each ABS u by the following equation:

$$\phi_s[t+1] = \phi_s[t] + \rho(\tilde{\boldsymbol{\omega}}_s - \tilde{\mathbf{p}}_s). \quad (95a)$$

C. Coastline Base Stations Energy Efficiency (CBSs-EE)

This section deals with the CBSs EE maximization problem (62) by utilizing the same previous algorithms. Firstly, BD will apply to decompose, and then DA will transform the subproblem objective into a subtractive form. After that, ADMM will solve the subproblem, which is given as follows:

1) *Bender Decomposition for CBSs-EE*: Firstly, the loop counter, i.e., $i_c = 1$ is initialized. Then the variables \mathbf{a}_c for U ABS and M_h HUEs association is initialized with the upper bound $a_{\text{UB}} = 1$ lower bound $a_{\text{LB}} = 0$. Moreover, the function χ_c as an auxiliary variable, representing the objective function of a subproblem within the master problem's objective function, whose unitize value can be set as $\chi_c = 10^{-6}$ to avoid an unbounded solution.

Subproblem: We can express the dual variable for the ABSs and HUEs association i.e., $\kappa_{c,u}$ and κ_{c,m_h} respectively. Thus, the subproblem can be define as:

$$\max_{\mathbf{p}_c} \tilde{\eta}_c, \quad (96a)$$

$$\text{s.t. } \tilde{\eta}_c = \frac{R_c(\tilde{\mathbf{a}}_c, \mathbf{p}_c)}{P_c^+}, \quad (96b)$$

$$\mathbf{a}_{c,u} = \mathbf{a}_{c,u}^{i_c} : \kappa_{c,u}^{i_c}, \quad \forall c \in \mathcal{C}, \forall u \in \mathcal{U}, \quad (96c)$$

$$\mathbf{a}_{c,m_h} = \mathbf{a}_{c,m_h}^{i_c} : \kappa_{c,m_h}^{i_c}, \quad \forall c \in \mathcal{C}, \forall m_h \in \mathcal{M}_h, \quad (96d)$$

$$(49), (52), (53). \quad (96e)$$

Convergence Analysis and Bounds: The objective function at iteration i_c provides the upper bound, which is stated as:

$$\eta_{\text{UB}}^{i_c} = \frac{\tilde{R}_c(\mathbf{a}_{c,u}^{i_c}, \mathbf{p}_c^{i_c})}{\tilde{P}_c(\mathbf{a}_{c,u}^{i_c}, \mathbf{p}_c^{i_c})^+}. \quad (97)$$

The lower bound can be define as follows:

$$\eta_{\text{LB}}^{i_c} = \chi_c^{i_c}. \quad (98)$$

Thus, the stopping criterion can be stated as:

$$\begin{cases} \eta_{\text{UB}}^{i_c} - \eta_{\text{LB}}^{i_c} \leq \epsilon, & \text{stop,} \\ \text{otherwise,} & \text{continue,} \end{cases} \quad (99)$$

Master Problem: The loop counter update as $i_c = i_c + 1$, and after that the solvable problem become as follows:

$$\max_{\mathbf{a}_c, \chi_c} \chi_c, \quad (100a)$$

$$\text{s.t. } (46), (47) \quad (100b)$$

$$\chi_c \leq \eta_{\text{UB}}^{i_c} + \sum_{c=1}^C \sum_{u=1}^U \kappa_{c,u}^{i_c} (\mathbf{a}_{c,u} - \mathbf{a}_{c,u}^{i_c}) + \sum_{c=1}^C \sum_{m_h=1}^{M_h} \kappa_{c,m_h}^\psi (\mathbf{a}_{c,m_h} - \mathbf{a}_{c,m_h}^{i_c}), \quad (100c)$$

$$\chi_c \geq \chi^{\text{down}}, \quad (100d)$$

2) *Dinkelbach Algorithm for CBSs-EE*: The objective function in the satellite subproblem can be transformed as follows:

$$F(\mathbf{a}_c, \mathbf{p}_c; \eta_c) = R_c(\tilde{\mathbf{a}}_c, \mathbf{p}_c) - \eta_c P_c^+. \quad (101)$$

Thus, the equivalent optimization problem in subtractive form is reformulated as:

$$\begin{aligned} \max_{\mathbf{p}_c} & F(\tilde{\mathbf{a}}_c, \mathbf{p}_c; \eta_c), \\ \text{s.t.} & (49), (52), (53). \end{aligned} \quad (102)$$

3) *ADMM for CBSs-EE*: In this subproblem, we introduce an auxiliary variable ω_c as a global copy, which implies that a new equality constraint is applied to the subproblem (102), which can be given as:

$$\mathbf{p}_c = \omega_c. \quad \forall c \in \mathcal{C}. \quad (103a)$$

We can find that constraints (52) and (53) are involved in each CBS c . The corresponding subproblem (102) is then reformulated as:

$$\max_{\mathbf{p}_c, \omega_c} F(\tilde{\mathbf{a}}_c, \mathbf{p}_c; \eta_c), \quad (104a)$$

$$\text{s.t. } 0 \leq a_{c,u} \omega_{c,u}(n) \leq p_{\max}, \quad \forall c, u, \quad (104b)$$

$$0 \leq a_{c,m_h} \omega_{c,m_h}(n) \leq p_{\max}, \quad \forall c, m_h, \quad (104c)$$

$$(49). \quad (104d)$$

The problem's augmented Lagrangian function can be define as follows:

$$\mathcal{L} = F(\tilde{\mathbf{a}}_c, \mathbf{p}_c; \eta_c) + (\phi_c (\mathbf{p}_c - \omega_c)) + \frac{\rho}{2} (\|\mathbf{p}_c - \omega_c\|_2^2) \quad (105)$$

We consider that the global copy variables ω_c are managed by the central controller, and the variables \mathbf{p}_c are processed locally by each CBS c . Based on the above analysis, the global consensus problem for finding global variables ω_c is formulated as follows:

$$\min_{\omega_c} F(\tilde{\mathbf{a}}_c, \mathbf{p}_c; \eta_c) + (\phi_c (\tilde{\mathbf{p}}_c - \omega_c)) + \frac{\rho}{2} (\|\tilde{\mathbf{p}}_c - \omega_c\|_2^2), \quad (106a)$$

$$\text{s.t. } 0 \leq a_{c,u} \omega_{c,u}(n) \leq p_{\max}, \quad \forall c, u, \quad (106b)$$

$$0 \leq a_{c,m_h} \omega_{c,m_h}(n) \leq p_{\max}, \quad \forall c, m_h, \quad (106c)$$

where $\tilde{\mathbf{p}}_c$ indicates the constant values which can be obtained by satellite' update. Therefore, to update \mathbf{p}_c , we need to solve the following problem at each CBS:

$$\min_{\mathbf{p}_c} F(\tilde{\mathbf{a}}_c, \mathbf{p}_c; \eta_c) + (\phi_c (\mathbf{p}_c - \tilde{\omega}_c)) + \frac{\rho}{2} (\|\mathbf{p}_c - \tilde{\omega}_c\|_2^2), \quad (107a)$$

$$\text{s.t. } (49), \quad (107b)$$

where $\tilde{\omega}_c$ indicates the fixed value which can be obtained by central controller's update. Therefore, the dual variable ϕ_c can be updated at each CBS c by the following equation:

$$\phi_c[t+1] = \phi_c[t] + \rho (\tilde{\omega}_c - \tilde{\mathbf{p}}_c). \quad (108a)$$

In the next part, we examine the operation and complexity of algorithms for the proposed problems.

VI. SUMMARY AND COMPLEXITY ANALYSIS

As shown in Fig. 2, to solve the MINLP problem for the SAS-NTN networks, this framework consists of Bender decomposition, the Dinkelbach algorithm, ADMM, and an optimization solver. Bender's decomposition minimizes the complexity of solving the original MILNP by breaking it down into smaller, independent subproblems. Benders' cuts reduce feasible regions with no optimal solution in each iteration.

When using ADMM in a subproblem, it will produce an optimal solution in $O(1/\epsilon^2)$ iterations [68].

Furthermore, by analyzing the updates in each iteration, the needed complexity for each iteration may be determined. In the ABS EE scenario, updating the power and coordinates requires $O(U \times M_l)$, where U and M_l represent the ABSs and their associated LUEs, respectively. We utilize the convex solver to find a solution because there is no closed-form solution for calculating these variables. As a result, the complexity of these variable update iterations is determined by the solver and the platform employed. Following that, the global update requires $O(U)$ as a projection function, resulting in linear complexity. Finally, we have a constant complexity specified as $O(3)$ for the update of dual variables. It is worth noting that because the number of ABSs U is so small in comparison to the number of LUEs M_l we may ignore it. As a result, the worst-case complexity for a single loop is $O(U \times M)$. If Γ is the maximum number of iterations required to reach a sub-optimal solution, then the total execution time of the algorithm is $\Gamma \times O(M \times K)$. This suggests that by adjusting the parameters of ϵ , U , and M_l our technique can converge within a certain time limit. This same process of complexity analysis is applicable to satellite EE and CBS EE solutions [69].

VII. SIMULATION RESULTS AND ANALYSIS

We now evaluate the performance of our proposed framework. We investigate one random commerce route in the international seas between five ports for HUE travel that is around 500 km in length. Each port has one CBS that connects the port and the neighboring region to the users. Similarly, LUEs, i.e., fishermen and private boats, are taken into account in these territories up to a 20 km region in the sea. However, because of LoS linkages and low-gain antennas, these LUEs rely on ABSs for connectivity. As a result, 10 ABS are stationed in this location, traversing their predetermined course over the sea route for LUEs. As stated in [70], we assume that worldwide satellite coverage is accessible over the whole studied period of this network.

We consider a 1000 km x 1000 km square region with 50 HUEs spread randomly and equally for our simulations. In the case of LUEs, we assess their dispersion along the neighboring shoreline, where there are 50 of them and their distribution is random and uniform in a 20 km x 20 km square area. All five CBS under consideration are located near the coast, approximately 500 km apart. At a height of 200 km, the satellite is deemed in orbit, and all ABSs are initially released into the aerial field at a height of 30 meters. All statistical results are averaged over a large number of independent experimental iterations in which the initial locations of the LUEs and HUEs are randomized. All simulation results were conducted using Python. Gurobi [71] is an optimizer that is used to solve all optimization problems. Although the simulation does not cover all conceivable circumstances in real-world networking, the results offer an overview of the utility of our proposed strategy. The remaining main parameters are shown in Table II.

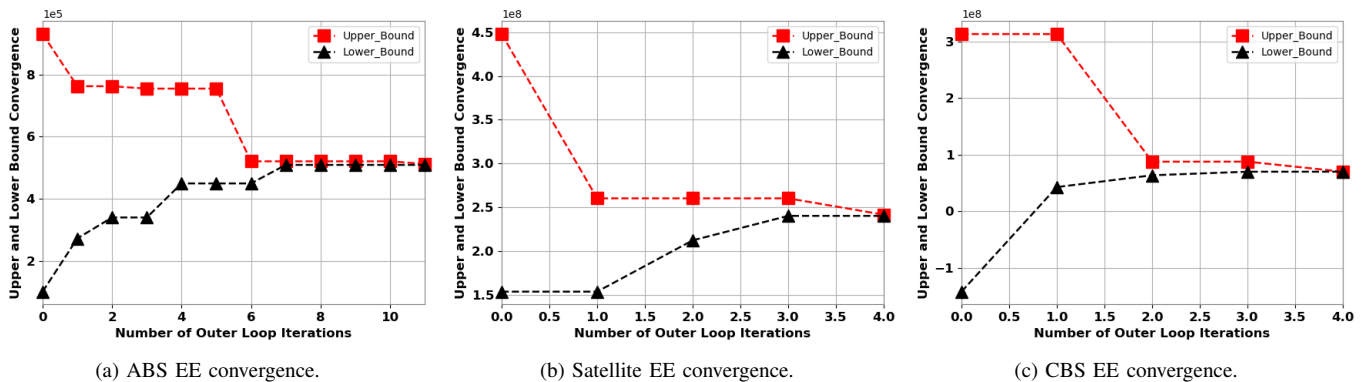


Figure 3: Illustration of the convergence results of three problems i.e., ABS EE, satellite EE, and CBS EE.

Table II: Simulation Parameters

Parameters	Values
CBS radius	100 km
Feasible lower bound	$\chi_{\text{down}} = 10^{-6}$
Maximum transmit power	$P_{\text{max}} = 33$ dBm
Noise power spectral density	$N_0 = -174$ dBm/Hz
Carrier frequency	$f = 30$ GHz
Satellite and CBS bandwidth	$B_s, B_c = 10$ MHz
ABS bandwidth	$B_u = 10$ KHz
Rician fading channel parameter	$\beta = 1.53$
HUE Antenna Gain	$G_i = 25$ dBi
UAV Antenna Gain	$G_u = 25$ dBi
Standard deviation	$\delta_u, \delta_{m_h}, \delta_c = 0.1$
reference distance pathloss	$\omega_{s,u}, \omega_{c,u}, \omega_{s,m_h} = 46.4$
pathloss exponent	$\zeta_{s,u}, \zeta_{c,u}, \zeta_{s,m_h} = 2$

Fig. 3 analyzes the convergence of our proposed algorithms for all three problems. The convergence of the ABSs' EE problems can be observed in Fig. 3a. The values of upper bound and lower bound are the optimization goals of the subproblem and master problems, respectively. According to Fig. 3, the value of the upper bound is always more than the ideal value, whereas the value of the lower bound is always less than the optimal value. The BD method can converge and approach the suboptimal solution. It can be observed that the BD algorithm for ABS EE converges to a suboptimal solution within 11 iterations. The convergence of satellite EE problems can be found in Fig. 3b. This problem also converged to a suboptimal solution with four iterations. This problem converges more quickly than the ABSs' EE problem due to fewer problem's information sharing with the network controller. Similarly, the convergence of CBS EE is presented in Fig. 3c. This problem also converges rapidly due to less amount of information sharing among network operator and each CBSs. This problem also converges to a suboptimal solution within four iterations.

We compared our results with four baseline algorithms, which can be defined as follows:

- **Centralized Algorithm:** This method, which has a complexity of $O(N \times \log(N))$, requires a coordinator and demands the entire information as inputs for addressing the defined problem in a centralized way. This scheme can be considered as its results achieve an optimal solution.
- **Greedy Algorithm:** We may use this technique to develop a locally optimal solution that approximates the

globally optimal solution at each iteration. In contrast, the greedy algorithm cannot guarantee a globally optimum solution. The algorithm's level of complexity is $O(N^2)$ [69].

- **Random Algorithm:** This method is distinguished by its degree of unpredictability, which employs uniform random distributions as inputs to achieve excellent performance in terms of average values over all potential input options.
- **Dynamic Programming:** A basic approach that takes into account all of the association and resource allocation pairings and returns suboptimal results. The algorithm's level of complexity is $O(N^2 \times \log N)$.

Fig. 4a compares our proposed ABS EE algorithms with the baselines. From this figure, we observe that, when the number of LUEs in the network is set to 10, the proposed algorithm provides the same outcomes as the centralized schemes. Moreover, when the number of LUEs in the network grows, the proposed algorithm produces near-optimal results due to interference and spectrum division in the network. However, the proposed approach outperforms the greedy, random, and dynamic allocation-based algorithms for any number of LUEs. Furthermore, as the number of LUEs associated with the ABSs grows and more bits move through this network, the total energy efficiency of the ABSs also increases, improving network performance. The proposed algorithm for ABS EE achieves up to 27%, 12%, and 7.7% when compared with random, greedy, and dynamic approaches, respectively, with the number of ABS is set to 10 and LUEs is set 50.

Fig. 4b evaluates the EE of the satellite. According to Fig. 4b, our technique achieves near-optimal results for any number of HUEs while the number of ABSs is fixed, which is set at 10 for satellite-based backhauling. However, under the same network setups, our technique outperforms the greedy, dynamic, and randomized allocation schemes. Furthermore, when the number of HUEs associated with the satellite increases, the network energy efficiency increases due to more data bits traveling across this network. The proposed algorithm for satellite EE achieves up to 16.5% and 57%, when compared with greedy and dynamic approaches, respectively, and the number of ABSs is set to 10 and HUEs is set to 50.

Fig. 4c shows how our proposed scheme for CBS EE

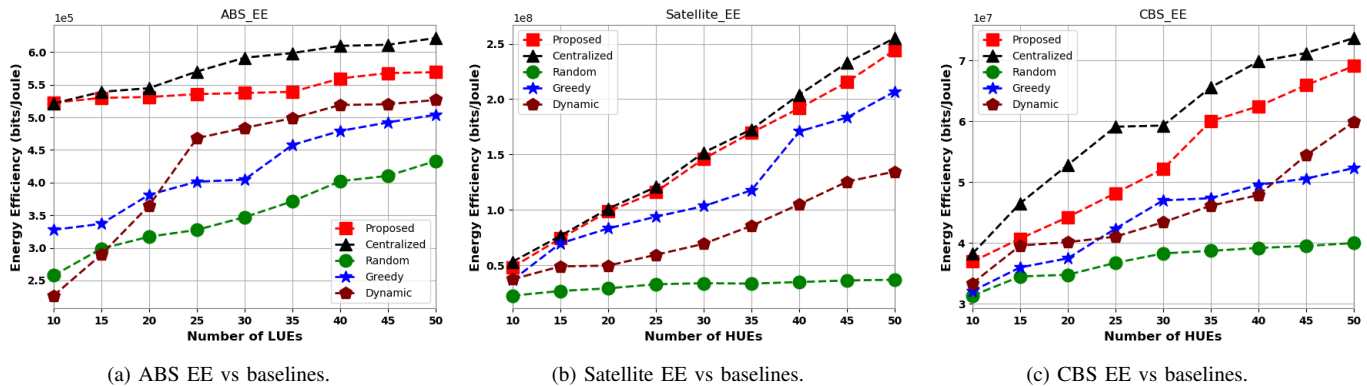


Figure 4: Illustration of our proposed algorithms comparison with two baselines for three problems i.e., ABS EE, satellite EE, and CBS EE.

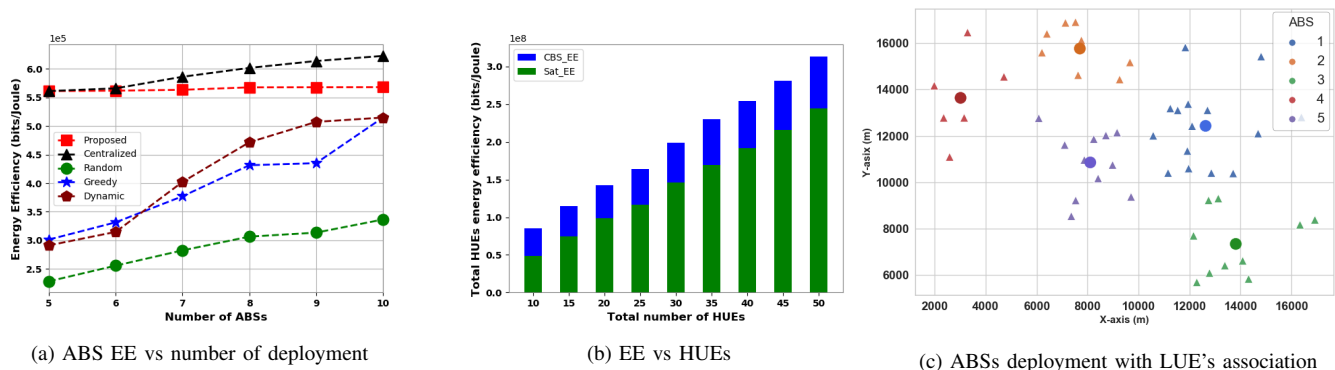


Figure 5: Illustration of the ABSs' EE, Sat EE, CBS EE, and ABSs' deployment.

relates to the other four baselines. It is demonstrated that the proposed schemes provide near-optimal results for any number of HUEs with a fixed number of ABSs, which is assumed to be 10. In this context, the proposed schemes outperform the randomized allocation schemes. Furthermore, as shown in Fig. 4c, when the number of HUEs in the network's surrounding region increases, the EE of the network improves because of an increased amount of bits traveling through the network, thus improving the overall CBSs network performance. The proposed algorithm for CBS EE achieves up to 27% 14.2% and 53.3% when compared with greedy, dynamic, and randomized approaches, respectively, and the number of ABSs is set to 10 and HUEs is set to 50.

We show in Fig. 5a how the number of ABSs deployed in the network affects the performance of ABS EE. We begin by deploying 5 ABSs in the selected zone and then increase them one by one to assess their impact. It can be shown that as the number of deployed ABSs in the network grows, so does the ABS EE. Furthermore, when the number of ABSs is low, the proposed methodology performs better at first since there is less interference in the system. The total system performs better as the number of ABSs increases gradually, but its relative results with centralized methods are lower due to more power consumption with ABS deployment. However, when compared to greedy, randomized, and dynamic schemes, our proposed algorithm achieves up to 9.8%, 51% and 9.83% respectively, with the fixed number of LUEs which is set to

50.

In Fig. 5b, we show how the EE of total HUEs relates to the satellite and CBS's. The satellite has a higher energy efficiency than CBS. This trend has two main reasons: satellites produce their energy from renewable energy sources such as solar energy, which is much less expensive than the running costs of CBS, and according to the system model, a satellite is a more viable network providing source in deep-sea waters than CBS because it can associate multiple HUEs, resulting in better results.

In Fig. 5c, we demonstrate the ABS deployment in the designated zone. The deployment of 5 ABSs, as well as the LUEs association, are depicted. The ABS positions are denoted by various colored circles. And the ground users are denoted by triangles of the same color as the connecting ABS. The ABS association depends upon the ABS EE maximization by taking into account all the QoS constraints as mentioned in the optimization problem (60).

VIII. CONCLUSION

In this article, we have studied a maritime wireless communication network that will be used to support future 6G networks. In this network, we designed a novel joint resource allocation of LUEs and HUEs, their association, transmit power control, and the ABSs' deployment problem. We then devised an optimization problem to improve the EE of deployed ABSs, satellites, and CBSs. We have proposed

a resource allocation algorithm framework based on joint Benders decomposition, the Dinkelbach algorithm, and the ADMM to handle this problem. This semi-distributed algorithm reduces the processing load on the network's controller while increasing system flexibility. Finally, simulation results show that our proposed method meets the convergence and performance requirements. Future research will investigate the energy and communication efficiency of integrating a larger number of satellites.

APPENDIX A PROOF OF LEMMA 1

We provide the Taylor approximation of the numerator in (55) with (68). We can define the first-order of the Taylor series as follows:

$$f(x_0) + f'(x_0)(x - x_0). \quad (\text{A.1})$$

Let assume $\mathbf{d}_{u,\text{local}}$ is local point of \mathbf{d}_u . Now, we can expand Taylor series for this function (55) at point $\mathbf{d}_{u,\text{local}}$. Before the Taylor series expansion, let's review a few logarithmic properties. The change of base rule can be given as:

$$\log_e x = \frac{\log_2 x}{\log_2 e}, \quad (\text{A.2})$$

it can be modified as:

$$\log_2 x = (\log_e x)(\log_2 e) = (\ln x)(\log_2 e), \quad (\text{A.3})$$

therefore, we replace the term x in the natural logarithm with the following term:

$$\ln \left\{ 1 + \frac{p_{u,m_i} g_0}{(\Omega_{u,m_i} + \sigma^2) \left(\left\| \mathbf{d}_u(n) - \mathbf{d}_{m_i}(n) \right\|^2 \right)} \right\}. \quad (\text{A.4})$$

Now, the derivative of natural the logarithmic function can be given as follows:

$$\frac{d(\ln[f(x)])}{dx} = \frac{1}{f(x)} f'(x). \quad (\text{A.5})$$

Now, let's take the derivative of the term given in (A.4) with respect to \mathbf{d}_u which is given in (A.6). After getting the derivative term, we can put all the terms in (A.2) to get the required expansion term of the objective function, which can be given in (A.7). We consider that $x_0 = \mathbf{d}_{u,\text{local}}$ is the local point around which the Taylor series is expressed. Similarly, we put the above-mentioned logarithmic identities in the expansion terms given in (A.7).

APPENDIX B PROOF OF LEMMA 2

We applied the Taylor series expansion to the quadratic safe distance constraint, which makes it linearize and can be solved with a standard solver. Here, we consider the local point $\mathbf{d}_{u,\text{local}}$ for each ABS around which the Taylor series applies. The first-order Taylor series can be expressed as:

$$f(x_0) + f'(x_0)(x - x_0). \quad (\text{B.1})$$

Here, function can be represented as:

$$f(\mathbf{d}_u) = \|\mathbf{d}_{u1} - \mathbf{d}_{u2}\|^2. \quad (\text{B.2})$$

We can simply the norm function as follows:

$$f(\mathbf{d}_u) = \langle \mathbf{d}_{u1} - \mathbf{d}_{u2}, \mathbf{d}_{u1} - \mathbf{d}_{u2} \rangle \quad (\text{B.3})$$

Let's take the first-order derivative of function (B.3) according to Leibniz formula which can be expressed as:

$$(uv)' = u'v + uv'. \quad (\text{B.4})$$

Lets put our function into the above the equation:

$$f(\mathbf{d}_u)' = \mathbf{d}_{u1} - \mathbf{d}_{u2} + \mathbf{d}_{u1} - \mathbf{d}_{u2}, \quad (\text{B.5})$$

which can be simplify as follows:

$$f(\mathbf{d}_u)' = 2(\mathbf{d}_{u1} - \mathbf{d}_{u2}), \quad (\text{B.6})$$

Lets combine all the terms and put in first order Taylor series as given in (B.1):

$$\|\mathbf{d}_{u1,\text{local}} - \mathbf{d}_{u2,\text{local}}\|^2 + 2(\mathbf{d}_{u1} - \mathbf{d}_{u2}) \cdot (\mathbf{d}_{u1,\text{local}} - \mathbf{d}_{u2,\text{local}}), \quad (\text{B.7})$$

which can be modified as follows by applying the dot product property of transposition:

$$\|\mathbf{d}_{u1,\text{local}} - \mathbf{d}_{u2,\text{local}}\|^2 + 2(\mathbf{d}_{u1,\text{local}} - \mathbf{d}_{u2,\text{local}}) \cdot (\mathbf{d}_{u1} - \mathbf{d}_{u2})^T. \quad (\text{B.8})$$

So this is the simplified first-order Taylor expansion of the safe distance quadratic constraint.

REFERENCES

- [1] W. Saad, M. Bennis, and M. Chen, "A vision of 6G wireless systems: Applications, trends, technologies, and open research problems," *IEEE Network*, vol. 34, no. 3, pp. 134–142, Oct. 2020.
- [2] M. Giordani, M. Polese, M. Mezzavilla, S. Rangan, and M. Zorzi, "Toward 6G networks: Use cases and technologies," *IEEE Communications Magazine*, vol. 58, no. 3, pp. 55–61, Mar. 2020.
- [3] S. Dang, O. Amin, B. Shihada, and M.-S. Alouini, "What should 6G be?" *Nature Electronics*, vol. 3, no. 1, pp. 20–29, Jan. 2020.
- [4] X. Li, W. Feng, Y. Chen, C. Wang, and N. Ge, "Maritime coverage enhancement using UAVs coordinated with hybrid satellite-terrestrial networks," *IEEE Transactions on Communications*, pp. 1–1, Jan. 2020.
- [5] D. Zhou, M. Sheng, X. Wang, C. Xu, R. Liu, and J. Li, "Mission aware contact plan design in resource-limited small satellite networks," *IEEE Transactions on Communications*, vol. 65, no. 6, pp. 2451–2466, Mar. 2017.
- [6] R. Sun, Y. Wang, R. Su, N. Cheng, and X. S. Shen, "A destination-aided wireless energy transfer scheme in multi-antenna relay sensor networks," *IEEE Wireless Communications Letters*, vol. 8, no. 3, pp. 689–692, June 2019.
- [7] N. Hossein Motlagh, T. Taleb, and O. Arouk, "Low-altitude unmanned aerial vehicles-based internet of things services: Comprehensive survey and future perspectives," *IEEE Internet of Things Journal*, vol. 3, no. 6, pp. 899–922, Dec. 2016.
- [8] R. Deng, B. Di, H. Zhang, L. Kuang, and L. Song, "Ultra-dense LEO satellite constellations: How many LEO satellites do we need?" *IEEE Transactions on Wireless Communications*, vol. 20, no. 8, pp. 4843–4857, 2021.
- [9] J. Jiang, S. Yan, and M. Peng, "Regional LEO satellite constellation design based on user requirements," in *Proc. of the IEEE/CIC International Conference on Communications in China (ICCC)*, Beijing, China, Aug. 2018, pp. 855–860.
- [10] C. Dai, G. Zheng, and Q. Chen, "Satellite constellation design with multi-objective genetic algorithm for regional terrestrial satellite network," *China Communications*, vol. 15, no. 8, pp. 1–10, Aug. 2018.

$$\begin{aligned}
\frac{\partial}{\partial \mathbf{d}_u} \ln \left\{ 1 + \frac{p_{u,m_i} g_0}{(\Omega_{u,m_i} + \sigma^2) \left(\left\| \mathbf{d}_u(n) - \mathbf{d}_{m_i}(n) \right\|^2 \right)} \right\} &= \left[\frac{1}{1 + \frac{p_{u,m_i} g_0}{(\Omega_{u,m_i} + \sigma^2) \left(\left\| \mathbf{d}_u(n) - \mathbf{d}_{m_i}(n) \right\|^2 \right)}} \right] \left[\left\{ \frac{p_{u,m_i} g_0}{(\Omega_{u,m_i} + \sigma^2)} \right\} \frac{\partial}{\partial \mathbf{d}_u} \left(\left\| \mathbf{d}_u(n) - \mathbf{d}_{m_i}(n) \right\|^2 \right)^{-1} \right] \\
&= \left[\frac{1}{(\Omega_{u,m_i} + \sigma^2) \left(\left\| \mathbf{d}_u(n) - \mathbf{d}_{m_i}(n) \right\|^2 \right) + p_{u,m_i} g_0} \right] \left[\left\{ \frac{p_{u,m_i} g_0}{(\Omega_{u,m_i} + \sigma^2)} \right\} (-1) \left(\left\| \mathbf{d}_u(n) - \mathbf{d}_{m_i}(n) \right\|^2 \right)^{-2} \right] \\
&= \left[\frac{-p_{u,m_i} g_0}{\left\{ (\Omega_{u,m_i} + \sigma^2) \left(\left\| \mathbf{d}_u(n) - \mathbf{d}_{m_i}(n) \right\|^2 \right) + p_{u,m_i} g_0 \right\} \left\{ (\Omega_{u,m_i} + \sigma^2) \left(\left\| \mathbf{d}_u(n) - \mathbf{d}_{m_i}(n) \right\|^2 \right)^2 \right\}} \right] \\
&= \left[\frac{-p_{u,m_i} g_0}{\left\{ (\Omega_{u,m_i} + \sigma^2) \left(\left\| \mathbf{d}_u(n) - \mathbf{d}_{m_i}(n) \right\|^2 \right) + p_{u,m_i} g_0 \right\} \left\{ \left\| \mathbf{d}_u(n) - \mathbf{d}_{m_i}(n) \right\|^2 \right\}} \right]
\end{aligned} \tag{A.6}$$

$$\left[\log_2 \left\{ 1 + \frac{p_{u,m_i} g_0}{(\Omega_{u,m_i} + \sigma^2) \left(\left\| \mathbf{d}_{u,\text{local}}(n) - \mathbf{d}_{m_i}(n) \right\|^2 \right)} \right\} - \frac{p_{u,m_i} g_0 \left\{ \left\| \mathbf{d}_u(n) - \mathbf{d}_{m_i}(n) \right\|^2 - \left\| \mathbf{d}_{u,\text{local}}(n) - \mathbf{d}_{m_i}(n) \right\|^2 \right\} \log_2 e}{\left\{ \left\| \mathbf{d}_{u,\text{local}}(n) - \mathbf{d}_{m_i}(n) \right\|^2 \right\} \left\{ p_{u,m_i} g_0 + (\Omega_{u,m_i} + \sigma^2) \left(\left\| \mathbf{d}_{u,\text{local}}(n) - \mathbf{d}_{m_i}(n) \right\|^2 \right) \right\}} \right] \tag{A.7}$$

-
- [11] Z. Liu, W. Guo, W. Hu, and M. Xia, "Delay minimization for progressive construction of satellite constellation network," *IEEE Communications Letters*, vol. 19, no. 10, pp. 1718–1721, Oct. 2015.
- [12] C.-Q. Dai, M. Zhang, C. Li, J. Zhao, and Q. Chen, "QoE-aware intelligent satellite constellation design in satellite internet of things," *IEEE Internet of Things Journal*, vol. 8, no. 6, pp. 4855–4867, Oct. 2021.
- [13] I. Meziane-Tani, G. Métris, G. Lion, A. Deschamps, F. T. Bendimerad, and M. Bekhti, "Optimization of small satellite constellation design for continuous mutual regional coverage with multi-objective genetic algorithm," *International Journal of Computational Intelligence Systems*, vol. 9, no. 4, pp. 627–637, June 2016.
- [14] T. Savitri, Y. Kim, S. Jo, and H. Bang, "Satellite constellation orbit design optimization with combined genetic algorithm and semianalytical approach," *International Journal of Aerospace Engineering*, vol. 2017, May 2017.
- [15] Z. Qu, G. Zhang, H. Cao, and J. Xie, "LEO satellite constellation for internet of things," *IEEE Access*, vol. 5, pp. 18 391–18 401, Aug. 2017.
- [16] X. Zhu and Y. Gao, "Comparison of intelligent algorithms to design satellite constellations for enhanced coverage capability," in *Proc. of the 10th International Symposium on Computational Intelligence and Design (ISCID)*, vol. 2, Hangzhou, China, Dec. 2017, pp. 223–226.
- [17] M. Mozaffari, W. Saad, M. Bennis, and M. Debbah, "Unmanned aerial vehicle with underlaid device-to-device communications: Performance and tradeoffs," *IEEE Transactions on Wireless Communications*, vol. 15, no. 6, pp. 3949–3963, Feb. 2016.
- [18] A. Pokkunuru, Q. Zhang, and P. Wang, "Capacity analysis of aerial small cells," in *Proc. of the IEEE International Conference on Communications (ICC)*, Paris, France, May 2017, pp. 1–7.
- [19] M. M. Azari, F. Rosas, K. Chen, and S. Pollin, "Joint sum-rate and power gain analysis of an aerial base station," in *Proc. of the IEEE Globecom Workshops (GC workshop)*, Washington, DC, USA, Dec. 2016, pp. 1–6.
- [20] R. Fan, J. Cui, S. Jin, K. Yang, and J. An, "Optimal node placement and resource allocation for UAV relaying network," *IEEE Communications Letters*, vol. 22, no. 4, pp. 808–811, Feb. 2018.
- [21] J. Lyu, Y. Zeng, R. Zhang, and T. J. Lim, "Placement optimization of UAV-mounted mobile base stations," *IEEE Communications Letters*, vol. 21, no. 3, pp. 604–607, Nov. 2017.
- [22] Y. Sun, T. Wang, and S. Wang, "Location optimization for unmanned aerial vehicles assisted mobile networks," in *Proc. of the IEEE International Conference on Communications (ICC)*, Kansas City, MO, USA, May 2018, pp. 1–6.
- [23] M. F. Sohail, C. Y. Leow, and S. Won, "Non-orthogonal multiple access for unmanned aerial vehicle assisted communication," *IEEE Access*, vol. 6, pp. 22 716–22 727, Apr. 2018.
- [24] J. Zhang, Y. Zeng, and R. Zhang, "UAV-enabled radio access network: Multi-mode communication and trajectory design," *IEEE Transactions on Signal Processing*, vol. 66, no. 20, pp. 5269–5284, Aug. 2018.
- [25] Y. Zeng, R. Zhang, and T. J. Lim, "Throughput maximization for UAV-enabled mobile relaying systems," *IEEE Transactions on Communications*, vol. 64, no. 12, pp. 4983–4996, Sep. 2016.
- [26] Q. Wu, Y. Zeng, and R. Zhang, "Joint trajectory and communication design for multi-UAV enabled wireless networks," *IEEE Transactions on Wireless Communications*, vol. 17, no. 3, pp. 2109–2121, Jan. 2018.
- [27] Y. Zeng and R. Zhang, "Energy-efficient UAV communication with trajectory optimization," *IEEE Transactions on Wireless Communications*, vol. 16, no. 6, pp. 3747–3760, Mar. 2017.
- [28] M. Hua, Y. Wang, Z. Zhang, C. Li, Y. Huang, and L. Yang, "Power-efficient communication in UAV-aided wireless sensor networks," *IEEE Communications Letters*, vol. 22, no. 6, pp. 1264–1267, Apr. 2018.
- [29] D. H. Choi, S. H. Kim, and D. K. Sung, "Energy-efficient maneuvering and communication of a single UAV-based relay," *IEEE Transactions on Aerospace and Electronic Systems*, vol. 50, no. 3, pp. 2320–2327, Apr. 2014.
- [30] P. Zhan, K. Yu, and A. L. Swindlehurst, "Wireless relay communications with unmanned aerial vehicles: Performance and optimization," *IEEE Transactions on Aerospace and Electronic Systems*, vol. 47, no. 3, pp. 2068–2085, July 2011.
- [31] F. Jiang and A. L. Swindlehurst, "Optimization of UAV heading for the ground-to-air uplink," *IEEE Journal on Selected Areas in Communications*, vol. 30, no. 5, pp. 993–1005, 2012.
- [32] J. Ouyang, Y. Zhuang, M. Lin, and J. Liu, "Optimization of beamforming and path planning for UAV-assisted wireless relay networks," *Chinese Journal of Aeronautics*, vol. 27, no. 2, pp. 313–320, Apr. 2014.
- [33] E. Kalantari, I. Bor-Yaliniz, A. Yongacoglu, and H. Yanikomeroglu, "User association and bandwidth allocation for terrestrial and aerial base stations with backhaul considerations," in *Proc. of the IEEE 28th Annual International Symposium on Personal, Indoor, and Mobile Radio Communications (PIMRC)*, Montreal, QC, Canada, Oct. 2017, pp. 1–6.
- [34] U. Challita and W. Saad, "Network formation in the sky: Unmanned aerial vehicles for multi-hop wireless backhauling," in *Proc. of the IEEE Global Communications Conference (GLOBECOM)*, Singapore, Dec. 2017, pp. 1–6.
- [35] Y. Chen, W. Feng, and G. Zheng, "Optimum placement of UAV as relays," *IEEE Communications Letters*, vol. 22, no. 2, pp. 248–251, Nov. 2018.
- [36] S. Zhang, H. Zhang, Q. He, K. Bian, and L. Song, "Joint trajectory and power optimization for UAV relay networks," *IEEE Communications Letters*, vol. 22, no. 1, pp. 161–164, Oct. 2018.
- [37] J. Lyu, Y. Zeng, and R. Zhang, "UAV-aided offloading for cellular hotspot," *IEEE Transactions on Wireless Communications*, vol. 17, no. 6, pp. 3988–4001, Mar. 2018.
- [38] R. Duan, J. Wang, H. Zhang, Y. Ren, and L. Hanzo, "Joint multicast beamforming and relay design for maritime communication systems," *IEEE Transactions on Green Communications and Networking*, vol. 4, no. 1, pp. 139–151, Oct. 2020.

- [39] C. Jiang, C. Jiang, L. Yin, and Y. Qian, "Joint backhaul and access link resource management in maritime communication network," in *Proc. of the IEEE Global Communications Conference (GLOBECOM)*, Abu Dhabi, United Arab Emirates, Feb. 2018, pp. 1–6.
- [40] Y. Xu, Y. Wang, R. Sun, and Y. Zhang, "Joint relay selection and power allocation for maximum energy efficiency in hybrid satellite-aerial-terrestrial systems," in *Proc. of the IEEE 27th Annual International Symposium on Personal, Indoor, and Mobile Radio Communications (PIMRC)*, Valencia, Spain, Sep. 2016, pp. 1–6.
- [41] T. Qi, W. Feng, and Y. Wang, "Outage performance of non-orthogonal multiple access based unmanned aerial vehicles satellite networks," *China Communications*, vol. 15, no. 5, pp. 1–8, June 2018.
- [42] M. Vondra, M. Ozger, D. Schupke, and C. Cavdar, "Integration of satellite and aerial communications for heterogeneous flying vehicles," *IEEE Network*, vol. 32, no. 5, pp. 62–69, Sep. 2018.
- [43] C. Joo and J. Choi, "Low-delay broadband satellite communications with high-altitude unmanned aerial vehicles," *Journal of Communications and Networks*, vol. 20, no. 1, pp. 102–108, Mar. 2018.
- [44] S. Zhang and J. Liu, "Analysis and optimization of multiple unmanned aerial vehicle-assisted communications in post-disaster areas," *IEEE Transactions on Vehicular Technology*, vol. 67, no. 12, pp. 12 049–12 060, Sep. 2018.
- [45] X. Zhang, W. Cheng, and H. Zhang, "Heterogeneous statistical QoS provisioning over airborne mobile wireless networks," *IEEE Journal on Selected Areas in Communications*, vol. 36, no. 9, pp. 2139–2152, Aug. 2018.
- [46] Y. Hu, M. Chen, and W. Saad, "Joint access and backhaul resource management in satellite-drone networks: A competitive market approach," *IEEE Transactions on Wireless Communications*, vol. 19, no. 6, pp. 3908–3923, Mar. 2020.
- [47] O. Semiar, W. Saad, and M. Bennis, "Joint millimeter wave and microwave resources allocation in cellular networks with dual-mode base stations," *IEEE Transactions on Wireless Communications*, vol. 16, no. 7, pp. 4802–4816, May 2017.
- [48] <https://www.searoutes.com/>.
- [49] M. Vondra, M. Ozger, D. Schupke, and C. Cavdar, "Integration of satellite and aerial communications for heterogeneous flying vehicles," *IEEE Network*, vol. 32, no. 5, pp. 62–69, Sep. 2018.
- [50] Z. Li, Y. Wang, M. Liu, R. Sun, Y. Chen, J. Yuan, and J. Li, "Energy efficient resource allocation for UAV-assisted space-air-ground internet of remote things networks," *IEEE Access*, vol. 7, pp. 145 348–145 362, Oct. 2019.
- [51] Y. Zeng and R. Zhang, "Energy-efficient UAV communication with trajectory optimization," *IEEE Transactions on Wireless Communications*, vol. 16, no. 6, pp. 3747–3760, Mar. 2017.
- [52] E. M. Greitzer, Z. S. Spakovszky, and I. A. I. A. Waitz, "Thermodynamics & propulsion, 16. unified, MIT course notes." July 2016. [Online]. Available: <http://web.mit.edu/16.unified/www/FALL/thermodynamics/>
- [53] U. Challita, W. Saad, and C. Bettstetter, "Interference management for cellular-connected UAVs: A deep reinforcement learning approach," *IEEE Transactions on Wireless Communications*, vol. 18, no. 4, pp. 2125–2140, Mar. 2019.
- [54] W. Khawaja, I. Guvenc, D. W. Matolak, U. Fiebig, and N. Schneckenburger, "A survey of air-to-ground propagation channel modeling for unmanned aerial vehicles," *IEEE Communications Surveys Tutorials*, vol. 21, no. 3, pp. 2361–2391, May 2019.
- [55] M. Bekhti, M. Abdennebi, N. Achir, and K. Boussetta, "Path planning of unmanned aerial vehicles with terrestrial wireless network tracking," in *Proc. of the Wireless Days (WD)*, Toulouse, France, Mar. 2016, pp. 1–6.
- [56] Y. Zeng and R. Zhang, "Energy-efficient UAV communication with trajectory optimization," *IEEE Transactions on Wireless Communications*, vol. 16, no. 6, pp. 3747–3760, Mar. 2017.
- [57] Y. Zeng, R. Zhang, and T. J. Lim, "Throughput maximization for UAV-enabled mobile relaying systems," *IEEE Transactions on Communications*, vol. 64, no. 12, pp. 4983–4996, Sep. 2016.
- [58] Z. Jia, M. Sheng, J. Li, D. Niyato, and Z. Han, "LEO satellite-assisted UAV: Joint trajectory and data collection for internet of remote things in 6G aerial access networks," *IEEE Internet of Things Journal*, pp. 1–1, Sep. 2020.
- [59] A. Ghosh, T. A. Thomas, M. C. Cudak, R. Ratasuk, P. Moorut, F. W. Vook, T. S. Rappaport, G. R. MacCartney, S. Sun, and S. Nie, "Millimeter-wave enhanced local area systems: A high-data-rate approach for future wireless networks," *IEEE Journal on Selected Areas in Communications*, vol. 32, no. 6, pp. 1152–1163, June 2014.
- [60] J. Wang, H. Zhou, Y. Li, Q. Sun, Y. Wu, S. Jin, T. Q. S. Quek, and C. Xu, "Wireless channel models for maritime communications," *IEEE Access*, vol. 6, pp. 68 070–68 088, Nov. 2018.
- [61] J. Faber, D. Nelissen, G. Hon, H. Wang, and M. Tsimplis, "Regulated slow steaming in maritime transport: An assessment of options, costs and benefits," *CE Delft. Delft, Netherlands*, 2012.
- [62] A. Pokkunuru, Q. Zhang, and P. Wang, "Capacity analysis of aerial small cells," in *Proc. of the IEEE International Conference on Communications (ICC)*, Paris, France, May 2017, pp. 1–7.
- [63] <https://www.gurobi.com/products/gurobi-optimizer/>.
- [64] A. J. Conejo, E. Castillo, R. Minguez, and R. Garcia-Bertrand, *Decomposition techniques in mathematical programming: Engineering and science applications*. Springer Science & Business Media, 2006.
- [65] L. Li, X. Wen, Z. Lu, W. Jing, and H. Zhang, "Energy-efficient multi-UAVs deployment and movement for emergency response," *IEEE Communications Letters*, pp. 1–1, Jan. 2021.
- [66] W. Dinkelbach, "On nonlinear fractional programming," *Management science*, vol. 13, no. 7, pp. 492–498, Mar. 1967.
- [67] Y. Yu, X. Bu, K. Yang, Z. Wu, and Z. Han, "Green large-scale fog computing resource allocation using joint benders decomposition, dinkelbach algorithm, ADMM, and branch-and-bound," *IEEE Internet of Things Journal*, vol. 6, no. 3, pp. 4106–4117, Oct. 2019.
- [68] T. Lin, S. Ma, and S. Zhang, "Iteration complexity analysis of multi-block ADMM for a family of convex minimization without strong convexity," *Journal of Scientific Computing*, vol. 69, no. 1, pp. 52–81, 2016.
- [69] S. M. A. Kazmi, T. N. Dang, I. Yaqoob, A. Ndikumana, E. Ahmed, R. Hussain, and C. S. Hong, "Infotainment enabled smart cars: A joint communication, caching, and computation approach," *IEEE Transactions on Vehicular Technology*, vol. 68, no. 9, pp. 8408–8420, July 2019.
- [70] P. Zong and S. Kohani, "Optimal satellite LEO constellation design based on global coverage in one revisit time," *International Journal of Aerospace Engineering*, vol. 2019, Dec. 2019.
- [71] L. Gurobi Optimization, "Gurobi optimizer reference manual," 2021. [Online]. Available: <http://www.gurobi.com>